PALAIOS
Emphasizing the impact of life on Earth's history

PALAIOS, 2018, v. 33, 185–203
Research Article
DOI: http://dx.doi.org/10.2110/palo.2017.091

EDIACARAN-STYLE DECAY EXPERIMENTS USING MOLLUSKS AND SEA ANEMONES

BRANDT M. GIBSON,[1] JAMES D. SCHIFFBAUER,[2,3] AND SIMON A. F. DARROCH[1]
[1]*Department of Earth and Environmental Sciences, Vanderbilt University, PMB 351805, 2301 Vanderbilt Place, Nashville, Tennessee 37235-1805, USA*
[2]*Department of Geological Sciences, University of Missouri, Columbia, Missouri 65211, USA*
[3]*X-ray Microanalysis Core Facility, University of Missouri, Columbia, Missouri 65211, USA*
email: brandt.m.gibson@vanderbilt.edu

ABSTRACT: **The latest Neoproterozoic Ediacara biota are a collection of enigmatic soft-bodied eukaryotes that have been variously interpreted as both diploblasts and triploblasts, and which are thought to have been preserved as pyritic 'death masks'. We perform decay experiments on sea anemones (*Condylactis gigantea*) and mollusks (*Dolabella auricularia*) under both 'normal' (i.e., baseline) and Ediacaran-style conditions; this allows us to construct decay indices for both these organismal groups, test the influence of Ediacaran taphonomic scenarios on rates and patterns of decay, and potentially constrain the phylogenetic affinities of Ediacaran fossils. We find that in both types of organisms the most labile tissues are preferentially lost, and tissue type exerts a stronger control on preservation than overall diploblastic versus triploblastic organization. Thus, in sum, there is not a large differential of preservation between diploblastic and triploblastic organisms. Geochemical analyses of sediment from around the carcasses indicate that pyritic 'death mask'-style preservation is dependent on the availability of Fe. Perhaps most importantly, experiments under Ediacaran-style taphonomic scenarios exhibit more rapid decay of labile tissues, such as anemone tentacles and the internal gut system of mollusks, than in baseline experiments. This finding highlights potential biases against the preservation of metazoan characters in the late Neoproterozoic, which may have influenced the interpretation of many iconic Ediacaran organisms.**

INTRODUCTION

The terminal Neoproterozoic Ediacara biota (575–541 Ma) is an enigmatic assemblage of large, morphologically complex eukaryotes that represents the first major radiation of multicellular life, and which may provide critical information surrounding evolutionary innovations in early complex life forms (Erwin et al. 2011). Organisms of the Ediacara biota were entirely soft bodied and possessed a variety of unusual morphologies that have no counterparts among extant animals. Most recent work suggests that they likely represent a polyphyletic grouping of several different eukaryotic lineages (Narbonne 2005; Xiao and Laflamme 2009; Darroch et al. 2015), although their unique body plans have led to them being collectively interpreted as occupying a variety of positions on the tree of life, including cnidarians (i.e., diploblasts; Hoffman 1990; Conway Morris 1993b), stem- and crown-group eumetazoans (mostly triploblasts, see e.g., Sokolov and Fedonkin 1984), protists (Zhuravlev 1993; Seilacher et al. 2003), lichens (Retallack 1994), fungi (Peterson et al. 2003), and an entirely separate Kingdom of eukaryotic life—the 'Vendobionta' (Seilacher 1989; Buss and Seilacher 1994).

Despite uncertainty in Ediacaran phylogenetic affinities, considerable strides have been made in understanding the mode in which these organisms were preserved. Fossils of the Ediacara biota are typically found as casts and molds, which historically have been attributed to the formation of pyritic 'death masks' (Gehling 1999). In this model, Ediacaran organisms lived in close association with thick, sediment-surface microbial mats, which were widespread in Neoproterozoic shallow-marine settings (Seilacher and Pflueger 1994; Seilacher 1999; Noffke et al. 2002; Noffke 2010). After death and rapid burial (e.g., during a storm event), aerobic decay depleted oxygen in the sediment surrounding the organism and isolated dysoxic-anoxic pore waters surrounding the carcass from oxygenated water above the sediment-water interface. Sulfate reducing bacteria (SRBs) were then able to convert sulfate (SO_4^{2-}) to hydrogen sulfide (H_2S), which in turn combined with ferrous iron (Fe^{2+}) in pore water to form a pyritic (FeS_2) 'death mask' that molded the external surface of the organism (Gehling 1999; Gehling et al. 2005; Droser et al. 2006).

Strong empirical evidence in support of this model has been discovered in a majority of Ediacaran fossil localities, and from a wide variety of facies settings. For example, in shallow marine sandstones from South Australia, iron oxides and oxyhydroxides (i.e., the oxidative weathering products of pyrite) are commonly found between bedding planes preserving fossils (Wade 1968; Tarhan et al. 2015; Liu et al. 2016). In addition, analyses of *Aspidella* in cross-section from the Fermeuse Formation, Newfoundland, uncovered pyrite and iron oxides disseminated within thin clay layers enveloping the fossils (Laflamme et al. 2011). Further, pyritized microbial filaments have been discovered in association with Ediacaran fossil deposits in Russia (Callow and Brasier 2009), and remineralized pyrite framboids have been described from deep water fossil surfaces associated with turbidite flows (Liu et al. 2015). In addition to empirical evidence from fossil surfaces, Darroch et al. (2012) were able to demonstrate incipient 'death mask' formation in decay experiments performed in the laboratory. Their study demonstrated a spatial association between Fe and S formed when organisms were decayed on microbial mats (although not in sufficient quantities to form the pyritic 'cement' around the outside of the organism envisaged in models), as well as the association of aluminosilicate-related cations (specifically K, Al, Fe, and Mg) with a dark-colored 'halo' that expanded and contracted around carcasses over the course of decay. This evidence for clay mineral formation also provided a close match with clay layers that have long been found associated with Ediacaran fossils, and from a wide range of localities worldwide (Wade 1968; Steiner and Reitner 2001; Mapstone and McIlroy 2006; Laflamme et

Published Online: May 2018
 0883-1351/18/033-185/$03.00

al. 2011; Meyer et al. 2012, 2014; Tarhan et al. 2014). On this basis, Darroch et al. (2012) suggested that authigenic clay layers, rather than pyrite, may be an important, early taphonomic control on molding soft-tissue morphology and eventual fossil formation in Ediacaran preservational scenarios.

The Darroch et al. (2012) study therefore provided preliminary support for some key aspects of the 'death mask' model, but also raised several additional questions, in particular the relative importance of iron sulfides versus clay minerals in molding the external surface of the decaying carcasses. In addition, their experiments had significant shortcomings, including the choice of *Galleria mellonella* (a crown-group triploblast and ecdysozoan arthropod possessing a chitinous cuticle) as a decay organism, the use of freshwater (rather than marine) microbial mats, and the fact that they did not quantify the extent of FeS formation. Effectively, the Darroch et al. (2012) experiments tested key tenets of the 'death mask' model, but were not designed in a way that allowed for more "actualistic" reinterpretation of Ediacaran fossils. Here, we expand upon that study in order to address the following questions:

(1) Do Ediacaran-style taphonomic scenarios affect the 'normal' (i.e., open marine) pattern and rate of decay?
(2) Do equivalent FeS 'death masks' form with both triploblastic and diploblastic organisms?
(3) Are the dark decay 'halos' that formed in the Darroch et al. (2012) experiments consistently associated with the precipitation of aluminosilicates?
(4) What is the rate and pattern of aluminosilicate precipitation as decay progresses?
(5) What is the relative importance of FeS versus clay minerals in molding the external morphology of carcasses, and thus in fossil preservation?

The answers to these questions allow a variety of potential interpretations surrounding the nature of Ediacaran organisms and paleoenvironments, the fidelity of Ediacaran 'death mask'-style experiments for interpreting Ediacaran fossils (see Briggs 2003; Sansom et al. 2010, 2011; Casenove et al. 2011; Nanglu et al. 2015; Briggs and McMahon 2016; McMahon et al. 2017) and broader-scale Ediacaran phylogenetic affinities (e.g., diploblastic or triploblastic), and the likelihood of development of pyrite (Gehling 1999; Schiffbauer et al. 2014; Cui et al. 2016) or clay minerals (e.g., Butterfield 1995; Orr et al. 1998; Anderson et al. 2011; Darroch et al. 2012) as controls for Ediacaran 'death mask'-style preservation.

METHODS

We conducted three sets of experiments. The first experiment was used to create a baseline for rate and pattern of decay. We then repeated our decay experiments under 'death mask'-style conditions in order to: (1) compare differences in the rates and patterns of character loss; and, (2) to compare the degree of incipient pyrite or aluminosilicate 'death mask' formation. Lastly, we conducted an Fe-supplemented experiment to assess a threshold amount of Fe required to precipitate FeS. To compare rates and patterns of FeS and aluminosilicate precipitation within any decay 'halos' that formed, we analyzed sediment from around the carcasses using scanning electron microscopy and energy dispersive x-ray spectroscopy analyses (SEM-EDS).

Decay Organisms

As decay organisms, we used the giant sea anemone *Condylactis gigantea* (a diploblast), and the wedge sea hare *Dolabella auricularia* (a triploblast). We chose these organisms because of their large size, ready availability, and relative structural simplicity. Both organisms possess few broad-scale morphological features that are unique to their species, and can reasonably be claimed to typify the anatomy of their broader taxonomic groupings (actinians and opisthobranch gastropods, respectively). In addition, both organisms belong to metazoan phyla that are thought to have been present among the Ediacara biota. Several authors have noted similarities between Ediacaran frondose organisms and sea anemones (Gehling 1991; Conway Morris 1993a, 2000; though see Laflamme and Narbonne 2008); *Inaria karli* (Gehling 1988) in particular is interpreted as a cnidarian of actinian grade. The presence of actinians in the latest Precambrian is supported by molecular divergence dates, which suggest a split between Anthozoa and Medusozoa in the Ediacaran (Erwin et al. 2011; Park et al. 2012). The justification for using *D. auricularia* as a decay organism is more complicated; no individual Ediacaran taxon has been specifically interpreted as an opisthobranch mollusk. Indeed, the earliest fossil examples of opisthobranchs are only from the Carboniferous (Pek et al. 1996). However, the bilaterian taxon *Kimberella quadrata* Glaessner and Wade 1966 is interpreted as a stem-group mollusk (Fedonkin and Waggoner 1997; Vinther 2015), possessing a muscular foot, lineations interpreted as dorsoventral musculature, and a structurally rigid (but non-biomineralized) carapace (Fedonkin and Waggoner 1997). Because opisthobranchs possess many of these characteristics, we consider *D. auricularia* as a reasonable modern analogue for *Kimberella*, and a plausible model organism for possible Ediacaran triploblasts. There are obvious associated caveats, however. *Dolabella* is larger than the vast majority of *Kimberella* specimens, and secretes a biomineralized posterior internal carapace, both of which are attributes which may influence patterns of decay. Additionally, we cannot rule out 'stemward slippage' artifacts to decay patterns (e.g., Sansom and Wills 2013) in either of these organisms.

***Condylactis gigantea* anatomy.**—Adult giant sea anemones, like most anemones, exist as polyps and are diploblastic organisms with radial symmetry. Figure 1 depicts the anatomy described here. They have an ectoderm and an endoderm, where the endoderm is differentiated into mesenteries, retractor muscles, pharynx, mesoglea, gametic tissue, and the gastrodermis. Like virtually all actinians, *Condylactis* has a radial oral disc surrounded by tentacles. This opening descends into a folding of the epidermis, known as the pharynx. The pharynx opens into the gastrovascular cavity, which is divided by multiple mesenteries. These mesenteries progress from the body wall toward the pharynx, with only some mesenteries connecting all the way to the pharynx.

***Dolabella auricularia* anatomy.**—Sea hares, mollusks similar to nudibranchs, are triploblastic organisms that have bilateral symmetry (Fig. 1). The external morphology of these organisms includes two rhinopores for sensing on the anterior end, a seminal groove between the anterior and posterior regions, and connecting incurrent and excurrent siphons on the posterior end. The anterior region is approximately one-third as narrow as the posterior region, which includes a calcareous shell that protects internal glands and gill from the incurrent via the siphonal flap. Musculature is arranged in a similar fashion to most marine opisthobranches, in which there are longitudinal somatic muscles running the length of the organism used for swimming.

Comparative Anatomy and Construction of Decay Indices.—We chose anatomical features to score for decay stages that were architecturally broad, which was done to facilitate easier comparisons with Ediacaran fossils (which in many localities tend not to preserve fine-scale anatomical details) as well as between decay organisms. These features included the anterior region, outer dermal layer, 'gut' tissue, and dorsoventral body tissue. These encompassed multiple smaller scale features that were described during the decay process, but that were

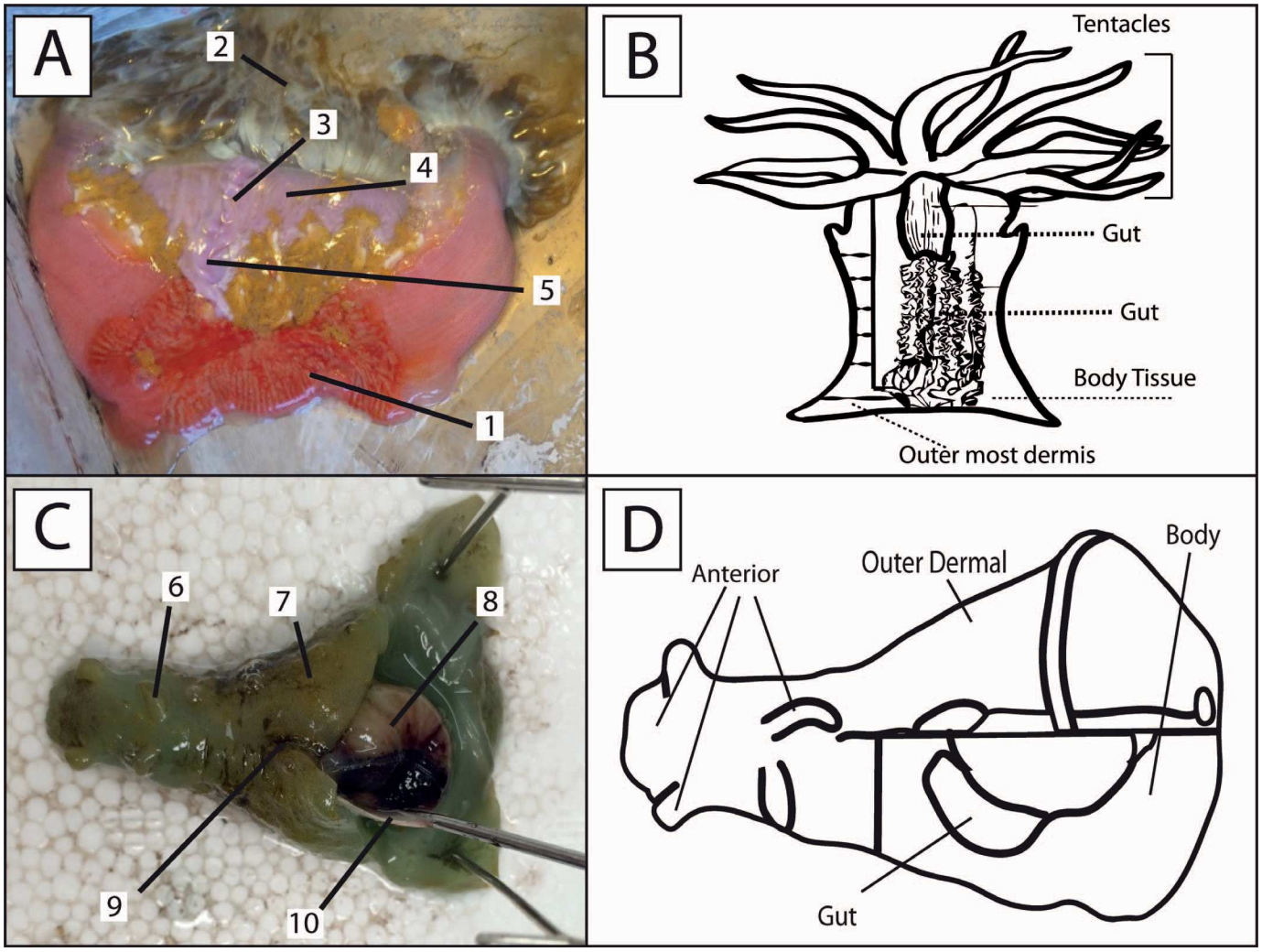

FIG. 1.—**A**) Image of *Condylactis gigantea*, the giant sea anemone, outlining anatomy. **B**) Generalized anatomical characters of *C. gigantea* used for decay indices. **C**) Annotated image of *Dolabella auricularia*, the wedge sea hare. **D**) Generalized anatomical characters of *D. auricularia* used for decay indices. 1 = pedal "foot", 2 = tentacles, 3 = pharynx, 4 = mesenteries, 5 = gametic tissue, 6 = rhinopore, 7 = outer dermis, 8 = gland, 9 = siphonal incurrent, 10 = posterior calcareous plate.

ultimately lumped into their respective groups (hereafter referred to as 'characters'). Anterior region characters included the tentacle region on *Condylactis*, and the head region of *Dolabella* containing the rhinopores. 'Gut' tissue in our anemones represents the gametogenic tissues as well as the pharynx. The same label was applied to the sea hare internal glands, gill, and various related organs. Body tissue character for the organisms included the mesenteries and muscles of the anemones and the locomotion muscles of the sea hares. Characters for both organisms are shown in Figure 1.

Decay indices (as categorical ranks) were generated by assigning a numerical decay state (DS) value to the characters described above, with each value representing proportional amount of anatomical loss. Values were scaled from 1 to 4 (DS1, DS2, etc.), with values of DS1 representing 0–25% loss of a specified feature, DS2, 25–50% loss, and so on. Observed features were generalized for easy comparison between diploblastic and triploblastic organisms (e.g., outer dermal layer, "gut", "body tissue", and "anterior region"). These indices are somewhat subjective, but are quick to assign, and are readily comparable with fossil material.

Decay Experiments

Baseline Decay Experiments.—We purchased decay organisms from an online aquarium retailer (see online Supplemental file). We euthanized organisms by placing them in a mixture of magnesium chloride hexahydrate ($MgCl_2*6H_2O$) and water at 50:50 ratio (Cameron 2002; Nanglu et al. 2015); this method has the advantage of not introducing foreign chemicals (which may affect either tissue lability or the composition of decay biota, Leary et al. 2013), but instead merely overdoses the organisms with the same chemical species they would naturally encounter in marine settings (Brusca 1980). To mitigate effects increased concentrations may have on the microbial biota, organisms were then rinsed with artificial seawater (ASW; specific gravity =1.02; see online Supplemental file), weighed, photographed, and placed in decay vessels. For decay vessels, we used 120 mL screw lid jars with 2 mm nylon mesh lining the bottom (modified from Nanglu et al. 2015). Mesh placement allowed for easier removal of carcasses and organic matter positioned at the bottom of decay vessels. Once specimens were deposited in vessels, ~ 60 mL of ASW were added to each vessel. Vessels were

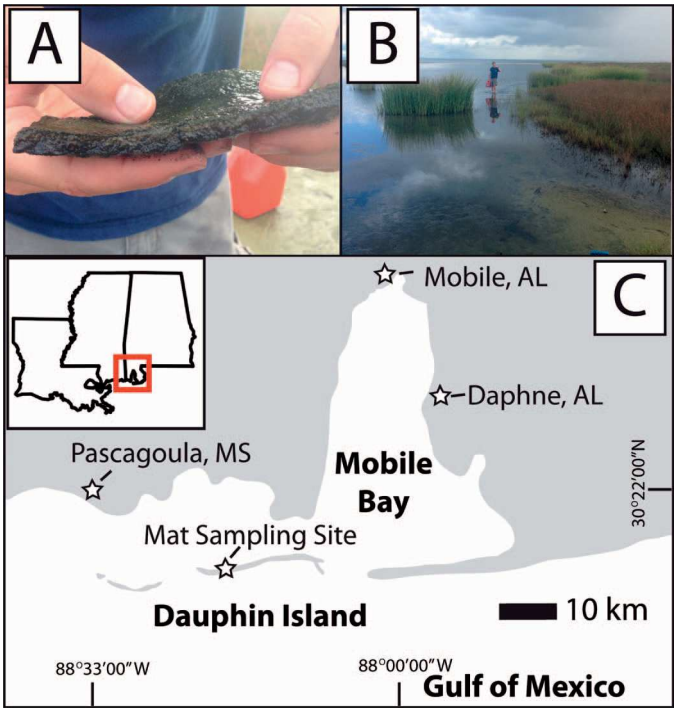

FIG. 2.—Location diagram of mat sampling site. **A**) Image of microbial mat showing green cyanobacterial top surface. **B**) Macroscopic view of mat sampling site. **C**) Map showing location of sampling site on sounds side of Dauphin Island, AL, in a large tidal pool (30°15′0.00"N/ 88°11′59.29"W).

sealed with lids and placed in a Heracell VIOS i160 tri-gas incubator to control for environmental conditions. Even though the vessels were sealed, we approximated extant atmospheric compositions 79% N, 0.1% CO_2, 21% O_2, and maintained a constant temperature of 25°C.

We sampled decaying organisms and observed the state/pattern of decay after 1, 2, 3, 4, 6, 8, 12, 17, 18, and 38 days. We chose sampling dates based on the rate of decay of the previous removal. To account for small differences in the size, weight, and characteristics of individual organisms, we sampled three individuals (hereafter referred to as 'replicates') per decay species at each interval. This resulted in decaying 33 individuals of each organism, or 66 organisms in total. Initial wet weights of all decay organisms are given in the online Supplemental file.

Upon extraction, water was pipetted off, and specimens were photographed before removal from their vessels. The same ASW was then carefully pipetted back into the appropriate vessel after the specimen had been returned being careful to attempt to not damage the specimens further. All three replicates were then frozen to -81°C for storage.

Ediacaran-Style Decay Experiments.—Following the same procedures as the baseline experiments, decay organisms were euthanized, rinsed, weighed, photographed, and prepared for decay experiments. For these experiments, decay vessels were 300 mL plastic rectangular storage containers; the larger size was necessitated by a more complicated experimental protocol.

Microbial mats were collected from the sound side of Dauphin Island, Alabama (30°15′0.00"N/ 88°11′59.29"W) (Fig. 2). The mat sampling locality is an estuarine tidal flat environment with medium grained, subangular quartz sand, underlying thick (~ 1 cm) microbial mats. Mats that accumulate here possess a typical redox stratification of microbial types and metabolisms, indicated by a green, cyanobacteria-dominated consortium near the top, and red- to purple-colored laminae underneath, characteristic of sulfur-redox bacteria (Vasconcelos et al. 2006) (Fig. 2). Mats were collected with the top few centimeters of underlying sediment to help maintain mat integrity during the removal and transport process. We also collected organic-poor sand (light colored sand not from directly underneath the mats) from nearshore of the sound side of the island, to use in simulating storm deposits in the experiments. Ocean water was also collected for inoculating the ASW used in the experiments to supply the mats with a medium as close to their native environmental conditions as possible. After inoculation, ASW was agitated and allowed to assimilate for 12-hours before added to the tank housing the microbial mats. It should be noted that as these materials were sampled from a naturally occurring saline environment; as such, they likely included associated invertebrate meiofauna.

The design of Ediacaran-style experiments broadly followed that of Darroch et al. (2012), which in turn mimics the storm-burial scenario described by Gehling (1999) for Ediacaran fossil surfaces in South Australia. A layer of sand was first placed in the bottom of the decay vessel. On top of this, we layered a section of mat (~ 1–2cm thick), and then placed decay specimens on top of the mat. In order to more easily split the vessels for sampling the decay specimens, sheets of plastic film (standard store-bought food wrap) were placed at the bottom of vessels as well as double layered on the tops of mats, with a circle cut out to allow: (1) contact between the decay organism and mat (see also Norris 1989) and (2) free transport of decay fluids and anions/cations around the decaying carcass. Remaining sand was then used to cover the decay specimens (~ 2 cm) to simulate storm deposited sediment. We saturated all decay vessels with inoculated ASW to prevent desiccation and better simulate a subtidal setting. Decay vessels were then sealed using plastic film to simulate the re-growth of microbial mats over the tops of storm beds (a step not performed by Darroch et al. 2012, but nonetheless a key part of the Gehling 1999 model). Vessels remained sealed throughout the duration of the experiment.

Ediacaran-Style Decay Stage Cataloging.—We removed three replicates per decay species after 1, 2, 5, 8, 13, 27, 34, 41, 56, 68, and 79 days, and immediately placed in them in a -81° C freezer to analyze specimens in a solidified form (see Darroch et al. 2012). After freezing, experiments were separated along the plastic wrap seams. The organisms were examined, photographed and scored for decay state using the same characters described in baseline experiments. In the event that a black precipitate was generated around the carcass, it was photographed and assessed to whether it extended part-way to the edge of the decay vessel or had filled the decay vessel entirely. Unfortunately, not all characters could be scored for each replicate due to the plastic wrap artificially biasing preservation of some characters. When plastic wrap inhibited the intersection of microbial mat and carcass, associated tissues were artificially preserved to almost pristine levels. These data were easily identified and removed prior to analyses.

Fe-Supplemented Experiments.—We assessed the possibility that sediment iron levels in our 'death mask'-style experiments were too low to precipitate pyrite precursors without supplemental Fe. Modifying the protocols discussed above, we mixed reduced iron (Fe) powder into the organic-poor sand (collected from nearshore) in concentrations of 0.1%, 1.0%, and 10% by total weight of sediment. At each level of Fe enrichment, one anemone was decayed under the same conditions as described before. All Fe-supplemented experiments were removed after 39 days.

SEM-EDS Analyses

All sediment analyses using scanning electron microscopy (SEM) and integrated energy dispersive X-ray spectrometry (EDS) were conducted at

TABLE 1.—*Sea anemone morphological character decay*.

Character (decay bin)	Description	Decay Index pattern of decay	Ediacaran-style decay pattern
Tentacles (anterior region)	Thin fluid-filled sacks used for stinging food	Rapidly lost	Rapidly lost, often turns into diffuse blob off tissue
Mesenteries (body tissue)	Longitudinal tissue that fully or partially connects to pharynx tissue	Most resistant to decay	Most resistant to decay
Outer-most dermis (outer dermal)	This layering of cells that usually appears clear above colored tissue around body	Initially turns vitreous, then sloughs off	Often diffuses into surrounding sediment, altering the coloration of the sediment
Foot (outer dermis/body tissue)	Thickest portion of the organism; provides structural support for attachment	Thickest, most cohesive tissue, persists	Often folded over itself, but also most likely to persist
Pharynx (gut)	Folded endodermis that attaches to the oral opening	Rapidly becomes less consolidated, but tissue material persists	Similar to Index Pattern, but maintains form for a much longer period of time
Gametic tissue (gut)	Internal, located near the foot	Rapidly lost, turns into diffuse liquid	Similar to pharynx, form is lost as diffuses into liquid

the University of Missouri X-ray Microanalysis Core Facility (MizzoμX). Sediment samples were selected from up to three locations within the decay replicates: (1) proximal to the decaying organism within the black-stained sediment of the decay halo; (2) at the interface between the visible decay halo and 'clean' sediment; and (3) from the distal 'clean' sediment. The sediments were prepared for SEM-EDS analyses, comparable to the methods used by Darroch et al. (2012), by affixing extracted sediments onto carbon disc adhesive-prepared aluminum stubs, with care taken to ensure nearly complete coverage of the adhesive. No conductive sputter-coating was applied.

Samples were analyzed using a customized Zeiss Sigma 500 VP SEM equipped with dual, co-planar Bruker XFlash 6|30 silicon drift detector (30 mm^2 active window) EDS systems. All imaging and X-ray spectroscopic analyses were conducted with identical operating conditions: low chamber vacuum (10 Pa); 19 keV beam accelerating voltage; high current mode (40 nA probe current); 60 μm aperture; and a sample working distance of 8.5 mm. Imaging was conducted with two different detectors: a high-definition five-segment backscattered electron detector (HDBSD; with the four radial segments positively biased and no bias on the fifth detector-arm segment) for compositional imaging; and a cascade current detector (C2D; with a 29.5% bias applied) for topographic imaging (measuring the resulting current from an ionization cascade through the chamber gas, N_2). The images represent a concurrent signal-mix from these two detectors (90:10 [HDBSD:C2D]). For area spectra, we utilized separate detection (with 15 seconds live time) for the EDS detectors, which resulted in two spectra which were then averaged. At the operating conditions used, the EDS detectors averaged $\sim$ 15–20k counts per second (kcps), with $\sim$ 20–30% dead time. Elemental mapping, with the co-planar EDS systems functioning together to provide a single map per region, was also conducted on each sample such as shown in Figure 3. Elemental mapping was conducted with a live time of 300 seconds and at slightly different operating conditions, including an accelerating voltage of 20 keV and 120 μm aperture, which yielded $>$ 200 kcps combined between the two detectors. Area spectra and elemental maps were collected from $\sim$ 4.5 $\times$ 3.4 mm regions that were densely covered in sediment. Maps were typically collected from the center of the stub unless there was not adequate coverage of sediment over the carbon tape. In these instances, field of view was repositioned to the nearest area with dense coverage of sediment (aiming for $\sim$ 80% coverage when possible). Spectra were ZAF corrected and quantified using the Bruker Esprit 2 software package, with compositional results reported in normalized weight percentage. In all cases, a large proportion of the carbon signal resulted from the mounting adhesive.

RESULTS

We first describe the rates and patterns of character loss in our baseline experiments; a more detailed and comprehensive list of these patterns specifically focusing on individual anatomical portions of the organisms can be found in Tables 1 and 2. We further compare and contrast these with the results of Ediacaran-style decay experiments, and finally describe the results of EDS analyses for the Ediacaran-style and Fe-supplemented decay experiments.

Baseline Decay Experiments

***Condylactis gigantea* (sea anemones).**—Decay in sea anemones generally progressed from anterior tentacle region to posterior foot. Time-series photos of typical progression of decay across example replicates (Fig. 4) and the overall pattern of decay of all replicates at each time step (Fig. 5) are provided. As shown in these figures, body tissue maintained structural integrity for the longest temporal range within the decay index. However, the thickest tissues of the anemone, the foot, persisted the longest, but were not specifically addressed in our index (see further caveats below). Tentacles were the first character to progress out of DS1, reaching DS2 by day two. All other decay characters persisted in DS1 until day five, at which point at least one replicate had transitioned to DS2. Following this pattern, tentacles were also the first tissues to progress into DS3 as well as into DS4, which first occurred on days five and nine, respectively. DS3 was observed in replicates up until the end of the experiment, indicating that DS3 and DS4 shared significant temporal overlap among replicates. Thicker tissues such as the mesenteries (body tissue), as well as the pharynx and gametic tissues ('gut' tissue), progressed at a slower rate. Body tissues fully transitioned to DS2 by day six, and the first replicate transitioned into DS3 on day seven. Although these two events appear temporally truncated, body tissues of at least one replicate remained in DS2 upon its removal on day 18. Body tissue never transitioned into DS4 throughout the entire experiment, while the gut tissues only made this transition at the end of the baseline experiment (day 38). Though these tissues did progress into DS4, they also exhibit a similar rate of loss and DS transition history to the mesentery tissues. Outer dermal tissue decay exhibited a different rate of decay than other tissues. This tissue category remained in DS1 for a similar length of time as the 'gut' and body tissue (last occurrence on day six), but DS2 was truncated compared to other tissues. Full transition from DS1 to DS3 took four days, and DS3 was observed even in the last set of replicates to be removed (day 38). DS4 first occurred on day 11, but some replicates did not progress to this stage by the end of the experiment.

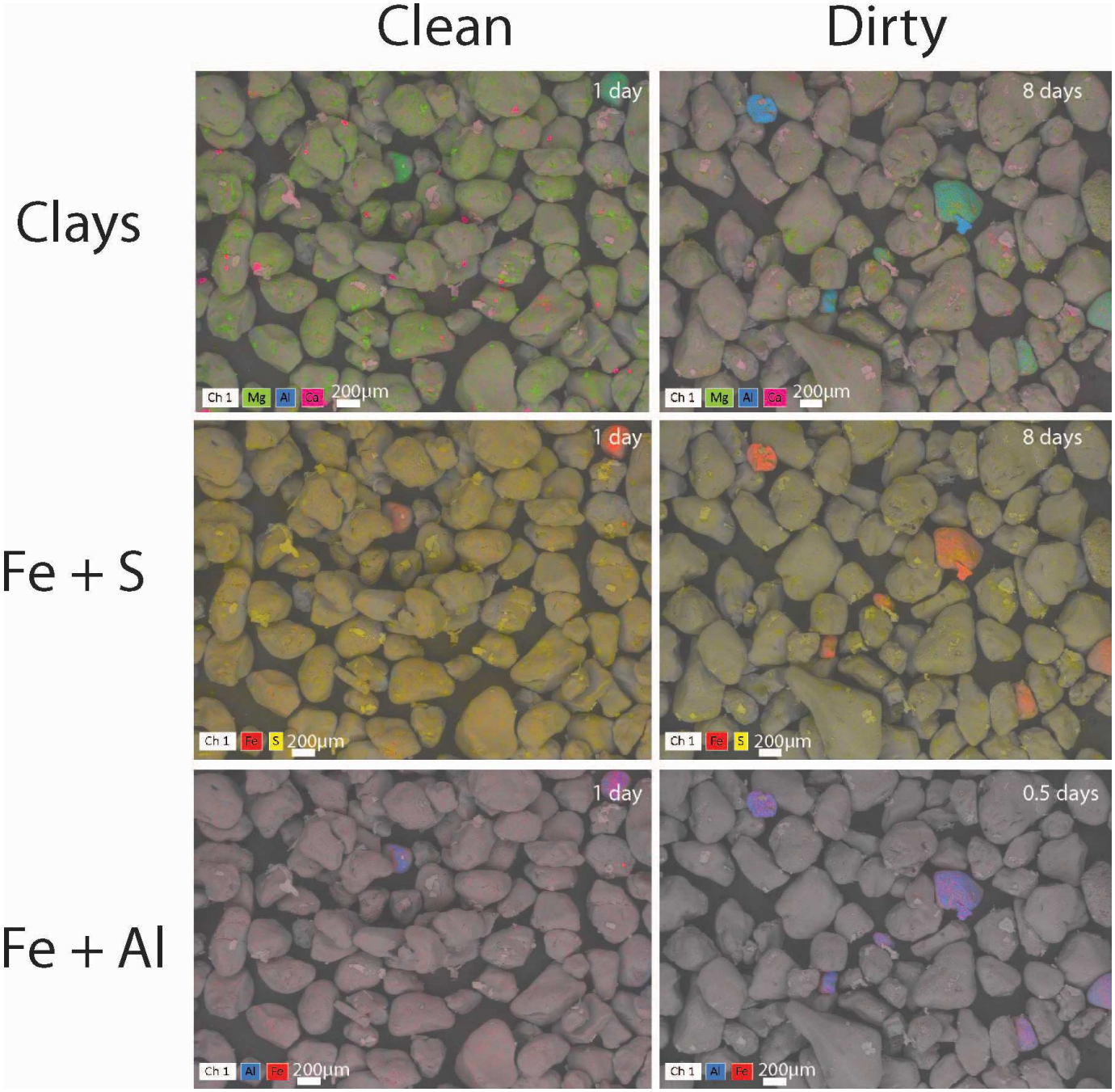

FIG. 3.—Elemental mapping of sediment samples from sea hare decay experiments. "Clean" sand indicating lack of progression of decay halo into it. "Dirty" indicating black precipitate has already progressed into this sediment region.

Some aspects of the decay progression were not assessed specifically in our decay indices, but were nonetheless noted. Immediately post-mortem, the fluids in the tentacles and much of the body cavity were ejected from the organism; this caused shrinking of the organisms, but this shrinking was temporally short-lived. By the first removal of decay replicates (day 0.5), fluids had diffused back into the organisms, eliminating their shrunken character. This is probably an artifact of the euthanizing process and left no observed permanent traces in the experiment. Furthermore, when left in the euthanizing solution, the anemones also everted a portion of their internal body cavity. This phenomenon also did not persist into the experiments and had disappeared by the first replicate removal (0.5 days). In addition, we noted that the sea anemone 'foot' was the most decay-resistant anatomical feature, although this part of the anatomy was not included in any of our scored characters. Lastly, the carcasses varied in buoyance throughout the decay window, most likely due to the production of decay-associated gases. Although initially at the base of the vessels, the carcasses became more positively buoyant for a temporary amount of time before returning to negative buoyancy and resting at the base of the vessels again. This usually occurred at day three and day 12 for positive and negative buoyancy, respectively.

TABLE 2.—*Sea hare morphological character decay*.

Character (decay bin)	Description	Decay Index pattern of decay	Ediacaran-style pattern of decay
Rhinopores (anterior)	Appendages of the head for sensory	Typically persists almost as long as overall out dermis	Often persists for as long as anterior region is present
Head (anterior)	Small portion of the body that houses the mouth and radula	As decays, it begins to tear and diffuse easily as compared to rest of carcass	Maintains structure much longer than baseline
Siphonal flap (body tissue)	Opening to internal anatomy, used for locomotion by moving water through	Opens as carcass bloats, then closes after gas is lost	Feature appears to be lost under Ediacaran conditions
Gill (gut)	Internal tissue protected by posterior shell; used for oxygen consumption	Rapidly is lost as turns to black sludge	Same pattern as baseline, but much slower rate
Longitudinal muscle (body tissue)	Used for locomotion, thicker tissues	Thins and diffuses out of siphonal flap	Persists long and disappears in conjunction with outer dermal tissue
Organs and glands (gut)	Used for reproduction and other physiological processes	Rapidly is lost as turns to black sludge along with gill	Same pattern as baseline, but much slower rate
Dermis (outer dermal)	Epidermis tissue that surrounds the organism	Typically persists after internal features have decayed	Typically decayed from ventral to dorsal, possibly due to position on mat

***Dolabella auricularia* (opisthobranch gastropods).**—Decay in the sea hares generally progressed outward from the carcass starting in the 'gut' (Fig. 5). Outer dermal tissues became translucent (Fig. 6) as the experiment progressed, and internal 'gut' tissues as well as internal tissues of the head darkened throughout decay. This was most evident by the end of the experiment as shown in day 18 (Fig. 6F). All characters in *D. auricularia* persisted in DS1 until day four, at which time all tissue regions in at least one replicate transitioned into DS2 (Fig. 5). That is not to say that the same replicate transitioned entirely into DS2 for all of its individually measured characters, rather transitions were staggered across replicates. Unlike the tentacle region in sea anemone experiments, the anterior region of the sea hares did not deteriorate more rapidly than other tissues. The anterior

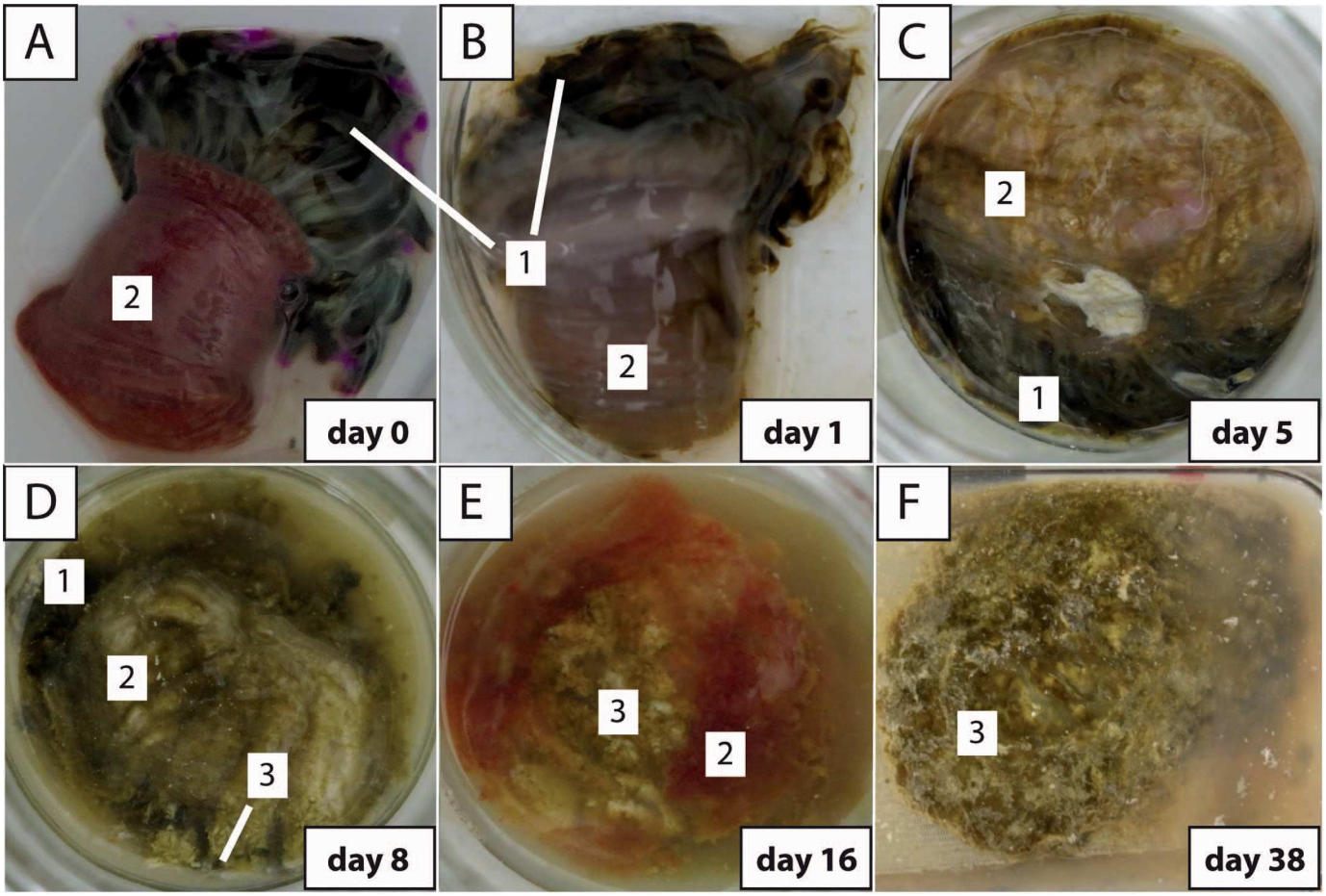

FIG. 4.—**A**–**F**) Progression of decay for giant sea anemone, *Condylactis gigantea*, under baseline conditions. Freshly euthanized sea anemone (A), tentacle diffusion after one day (B), tearing and liquification of tissue after five days (C), dissociation of tissues by day eight (D), pigmentation still present but tissues dissociated (E), all tissues dissociated (F). Legend: 1 = tentacles; 2 = body column; 3 = 'gut' material contracting and decaying from outer dermal layer.

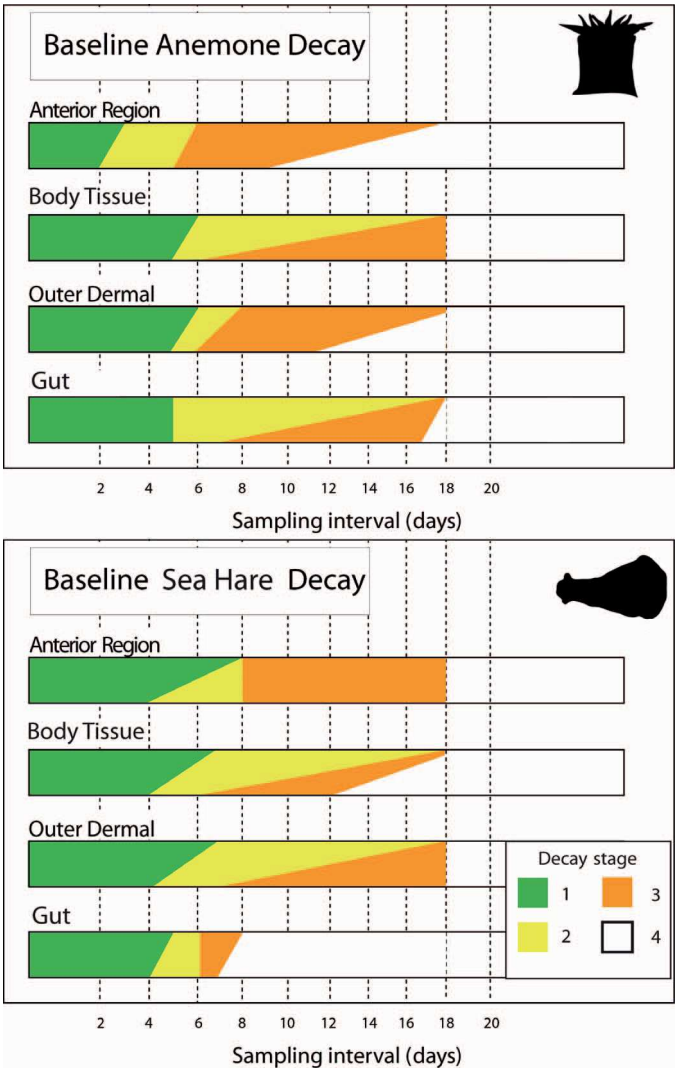

FIG. 5.—Pattern and temporal range of baseline-condition decay assessed from generalized decay characters. Top shows relative decay patterns for *Condylactis gigantea*, and bottom shows *Dolabella auricularia*. Colors indicate first and last observation of decay stag, such as Decay Stage 1 (DS1, green) indicates 0–25% loss of the decay character (e.g., "tentacles", " pharynx", etc.), DS2 indicates 25–50% loss, DS3 indicates 50–75% loss, and DS4 indicates 75–100% loss.

region of the sea hares progressed through DS2 at the same pace as other tissues and stayed in DS3 for the remainder of the experiment. During DS3, rhinopores were no longer individually discernable, but overall outline of the morphology was conserved (Fig. 6). Tissues of this region transitioned to DS3 by day eight and remained in DS3 until the end of the experiment. A similar pattern occurred with outer dermal tissues, which persisted in DS2 and DS3 from day four until the end of the experiment. Gut tissues of the sea hares, which consisted of the opaline gland, gill, and purple gland, were entirely lost by all specimens early on in the experiment. By day eight all evidence of these parts had been replaced by a black sludge typically located underneath the stiffened posterior plate (Fig. 6F). In the last set of replicates (day 18), two of the three experiments had progressed to DS4 with respect to the 'muscle' (see Methods, Comparative Anatomy and Construction of Decay Indices).

As with the anemones, some aspects of the decay experiments were not captured by our decay indices. Specifically, sea hares bloated early in the decay progression. This was most noticeable along the siphonal flap on the dorsal posterior portion of the organism. During bloating the interior body cavity of the organism was readily exposed, showing the gill and the calcareous shell (Fig. 6B). As decay progressed, bloating of the carcass decreased which was most noticeable by the siphonal flap closing, no longer leaving the internal anatomy exposed. Figure 7 illustrates these patterns of decay for both sea anemones and sea hares in a more visually comprehensive way.

Ediacaran-Style Decay Experiments

***Condylactis gigantea* (sea anemones).**—The pattern of character loss for sea anemones under Ediacaran-style death mask conditions (Figs. 8, 9) was very similar to that seen in baseline experiments (Figs. 4, 6). The rank of most decay-susceptible tissue to least decay-susceptible tissue was: anterior region (tentacles), gut tissue (gametic and pharynx tissue), outer dermal tissue, and body (mesentery) tissue. In the baseline experiments, outer dermal tissue was more susceptible to decay than gut tissue, which was reversed in the Ediacaran-analogue experiments. This reversed pattern should be accepted cautiously, though, because natural compaction of the organism during decay within the sediment/mat setting of the experimental vessels, as opposed to free submergence is ASW, made assigning DS values to internal tissues difficult. Furthermore, DS values for gut tissues and dermal tissues are very similar, with both tissue types exhibiting DS3 values for much of the experiment (days 8–68 and days 5–68, respectively).

Although patterns of decay were very similar, decay rates were vastly different between baseline and Ediacaran-analogue experiments. For the most part, Ediacaran-analogue experiment tissues transitioned into subsequent decay stages at a much slower rate than those under baseline conditions. Counter to this broad trend, the tentacles (anterior region) persisted for less time under Ediacaran conditions than baseline conditions (last observation of DS on day nine and 17, respectively). Although this increased decay rate of tentacles was counter to the overall delayed Ediacaran-type rate, the overall pattern of thinnest, most labile tissues being lost first was consistent across baseline and Ediacaran-style decay experiments.

As before, some aspects of the baseline decay experiments were not directly assessed in the decay indices. The foot of the sea anemones was again the most resistant feature to decay. This was further compounded by the additional factor of the tissues of the foot (1) folding over on itself and reducing exposed surface area, and (2) having the additional structural support provided by surrounding sediment. This structural support reduced the amount of stress on the tissues for falling apart. In baseline experiments, sea anemone carcasses maintained neutral to just negative buoyancy. As the replicates did not rest on the bottom of vessels during these experiments, they did not maintain shape as well during the decay processes. In these Ediacaran experiments, while body tissues persisted, they maintained shape much better than the baseline experiments. This trend is most evident in the foot and body tissues, though it should be noted that this may be affected by the folding over of tissue on itself in this region.

***Dolabella auricularia* (opisthobranch mollusks).**—In the same manner as *C. gigantea*, pattern of character loss in *D. auricularia* under Ediacaran-style death mask conditions (Figs. 9, 10) was very similar to that exhibited in baseline experiments (Fig. 5). The rank of most decay-susceptible tissue to least decay-susceptible tissue was: gut tissue, outer dermal tissue, anterior region (head), and muscle. The most notable difference in patterns between these two experiments was seen in the outer dermal layer, which was much more susceptible to decay under Ediacaran-style conditions. Under baseline conditions, outer dermal tissue was still present at the end of the experiment, while under Ediacaran conditions this tissue layer diffused into surrounding sediment beginning on day eight and

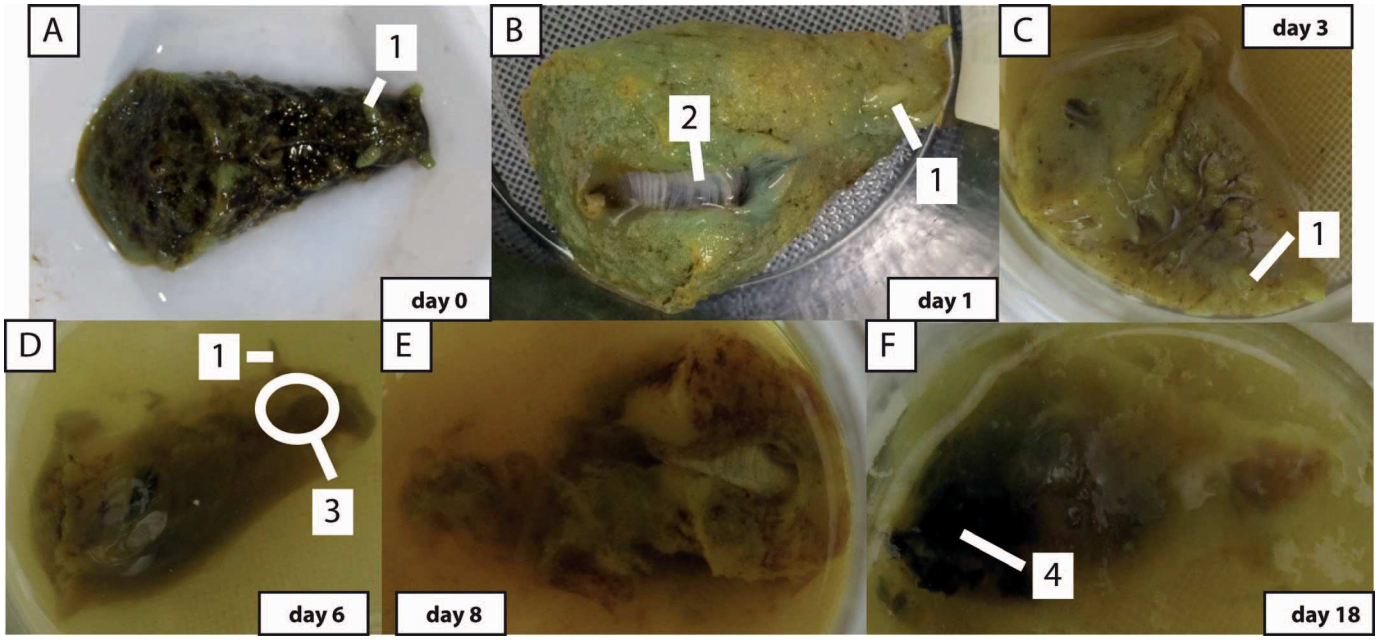

FIG. 6.—**A**–**F**) Progression of decay for wedge sea hare, *Dolabella auricularia*, under baseline conditions. Freshly euthanized sea hare (A), bloating with exposed internal shell (B), deflation of carcass (C), slight diffusion of tissues and moderate diffusion of pigment (D), tissues diffusing rapidly into surrounding media with lots of tearing in tissues (E), all tissues diffusing with only body outline still recognizable (F). Legend: 1 = rhinopores; 2 = calcareous shell; 3 = gut separating from outer dermal layer; 4 = gut leaching out becoming too decayed to discern further.

was entirely lost by day 41. Breaking down the patterns by character, muscle and dermal tissues persisted in DS3 for the majority of the experiment (days 13–56 and days 8–41, respectively). Sea hare muscle exhibited DS2 for a longer period than sea hare outer dermal tissue (days 2–35 and days 2–8, respectively). Lastly, pattern of tissue loss for the anterior region of sea anemone replicates was fairly mixed between those patterns for the muscle and dermal tissues. Replicates spent nearly equal time in DS2 and DS3 (days 2–27 and days 13–34, respectively) before transitioning entirely into DS4 on day 41 (where it remained for the rest of the experiment).

Similar to the sea anemones, *D. auricularia* decay rates were drastically slower than in baseline experiments. All characters transitioned into DS2 by day nine, and body tissues and anterior tissues did not fully transition into DS3 until day 36 (meaning DS2 was still noted in at least one replicate up until this point). The last reported DS3 values for body tissues and dermal tissues were days 56 and 41, respectively.

Black Decay 'Halos'.—In all replicates for both *C. gigantea* and *D. auricularia*, a black 'halo' became apparent within the sediments precipitating outward from the carcass, similar to that noted in Darroch

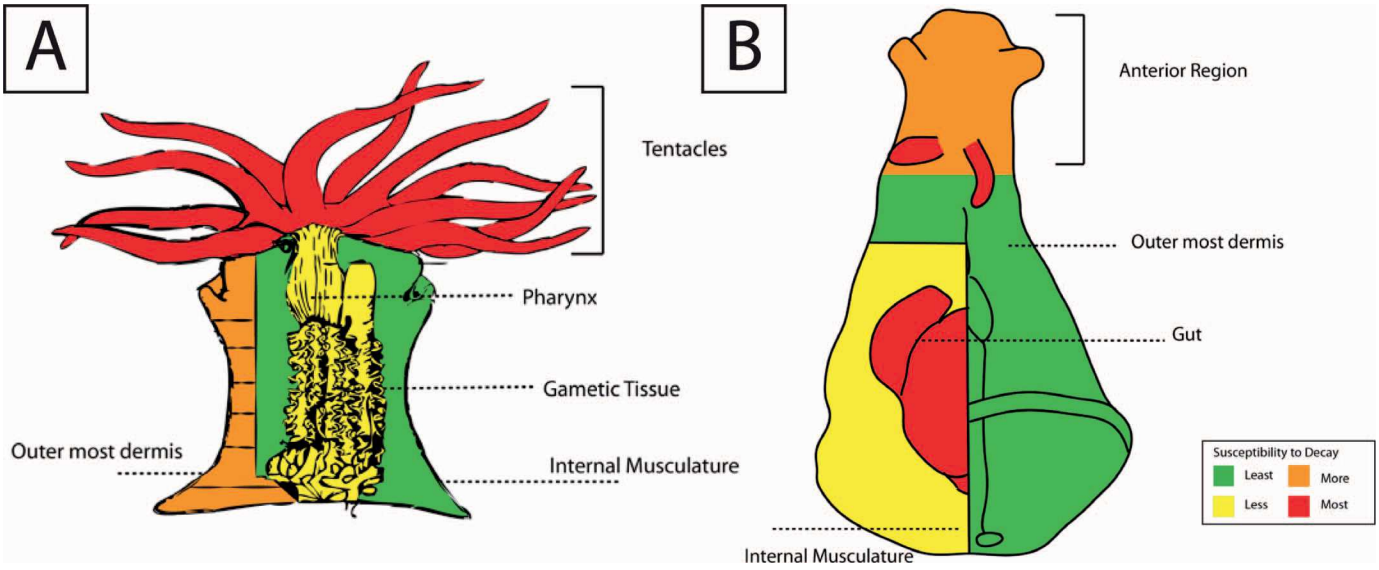

FIG. 7.—Decay indices for (A) sea anemones and (B) sea hares. Colors correspond to susceptibility of decay, where red is most susceptible and green is least susceptible.

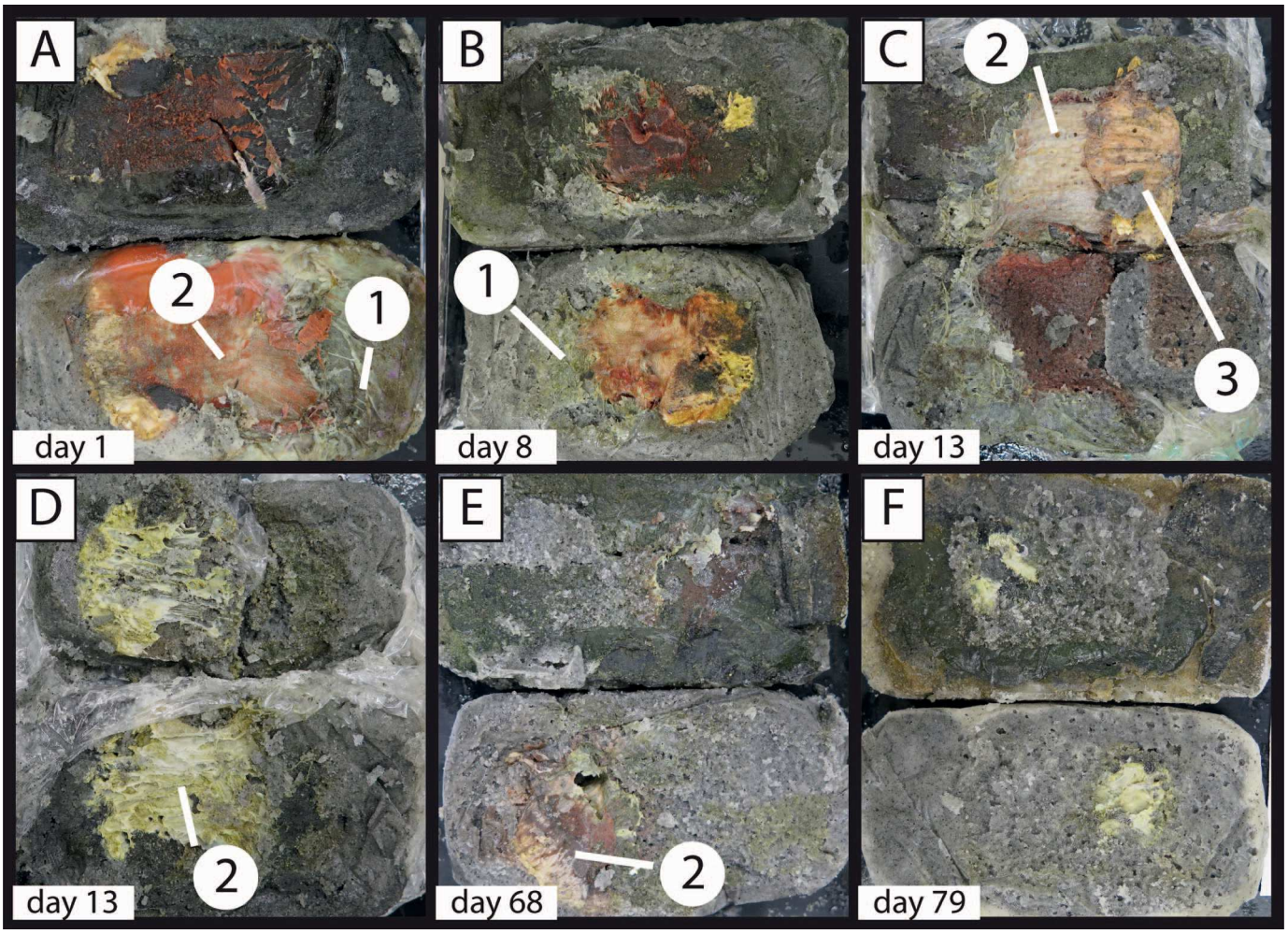

FIG. 8.—Progression of decay for giant sea anemone, *Condylactis gigantea*, under Ediacaran-style decay conditions. Labeled characters: 1 = remains of tentacles; 2 = remains of body muscle. **A**) Sea anemone decay progression after 24 hours. **B**) Tentacles almost lost after 8 days. **C**) Tentacles lost and foot preserving some tissue structure. **D**) Much of tissue has been lost by day 13. **E**) Although most tissue has decomposed, some still remains where the foot was located. **F**) Almost all tissue missing by day 79.

et al. (2012). The development and progression of these halos across sea hare replicates is shown in Figure 10. Decay halos appear at the start of experiments, after 12-hours in both organisms. By day nine, halos had entirely encompassed all of the decay vessels with no 'clean' sand visible. This progression occurred contemporaneously in both the sea anemones and sea hares. Halos persisted until the end of the experiment, at which point there was some contraction towards the carcasses in a few replicates, although no vessel entirely lost visible signs of the black precipitate.

To assess the composition of this material and its importance in 'death mask' style preservation, multiple sediment samples were analyzed via SEM-EDS from each decay vessel to track any changes that occurred throughout the temporal range of the experiment. Relative elemental mass abundances for each sample is provided in the online Supplemental file. Figure 11 shows the progression of Fe, S, Al, Mg, and Ca throughout the experiment, as well as tracking changes in each of these abundances by location of sediment sample.

SEM-EDS Analyses

Sediment samples were analyzed from the 66 decay replicates used in 'death mask'-style (n = 147) and Fe-supplemented 'death mask'-style (n = 9) decay experiments. 'Clean' sediment from prior to the onset of the decay experiments indicated a dominantly siliceous composition with abundant Mg, low K, and low Na. The enrichment of Mg was most likely due in part to the high Mg-concentrations of the ASW used to saturate the decay vessels for the duration of the experiment.

We analyzed our sediment samples in bins based on location of excavation relative to the carcass and the decay precipitate halo front. Sediment samples were broken down into four groups for each organism type: (1) decay halo sediment proximal to carcass; (2) sediment from the intersection of halo and 'clean' sand; (3) sediment entirely from 'clean' sand outside of the decay halo; and (4) sediment excavated from near the edge of the vessel when decay halos encompassed all of the sediment within their vessels. The abundances of elements are expressed as normalized weight percentages, which reflect the amount of each element observed in each elemental map where the sum of all observed elements equals ~ 100%. Changes in values from clean to 'dirty' sediment correspond to what is associated with presumed small-scale mineral precipitation on the sediment. Because we sealed vessels and did not supply additional ASW, there was finite amount of these elements with no replenishment possible. As such, changes in elemental concentrations from clean to 'dirty' sediment do not reflect variation in seawater, but instead reflect what is precipitating on sediment grains. These data are shown in Figure 11 and in the online Supplemental file.

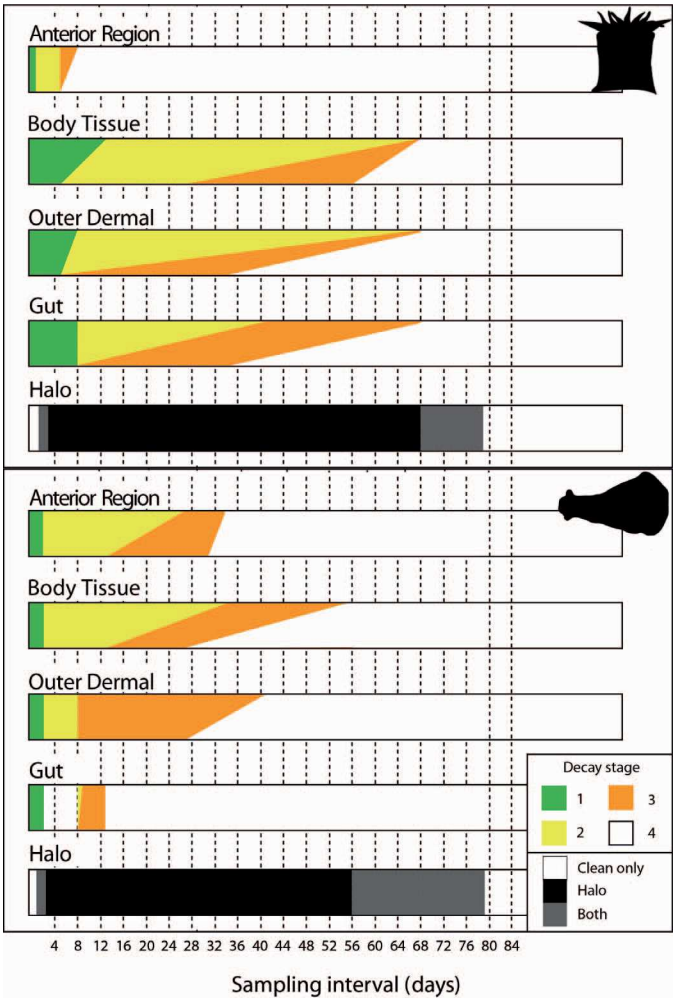

FIG. 9.—Pattern and temporal range of Ediacaran-style decay assessed from generalized decay characters. Top shows relative decay patterns for *Condylactis gigantea*, and bottom shows *Dolabella auricularia*. Colors indicate first and last observation of decay stag, such as Decay Stage 1 (DS1, green) indicates 0–25% loss of the decay character (e.g., "tentacles", " pharynx", etc.); DS2 indicates 25–50% loss; DS3 indicates 50–75% loss; and DS4 indicates 75–100% loss.

In all sediment groups for the Ediacaran-style decay experiments, there was little elemental concentration variation between groups (e.g., proximal to carcass, intersection point, etc.) (Fig. 11). Furthermore, concentrations remained fairly constant throughout the temporal duration of the experiment with some mild fluctuations in S and Mg for both sea anemones and sea hares. Specifically, within the decay halo, there were apparent spatial associations between Ca and Mg, Ca and Al, and Fe and Al. Associations between Fe and Al were more consistently associated with individual grains and preferentially with sea hares over sea anemones. In all sediment groups for both decay organisms, spatial associations between Fe and S were negligible at best. Sediment stub elemental maps show very little spatial co-occurrence of Fe and S, although S 'hot spots' are observed in much of the sea anemone 'clean' sediment, and occasionally in the decay halo sediment of the anemones. Additionally, Fe and Al regularly exhibit a spatial association (shown in Fig. 3), as do Ca and Mg as well as Ca and Al. The association of Fe and Al, which is typically found on specific grains with the sample, is very rarely widespread over the entire map. This occurs more consistently with the sea hares than with the sea anemones.

Fe-Supplemented Experiments.—Sediment from Fe-supplemented Ediacaran-style decay experiments demonstrated strong spatial associations between Fe and S, and resulted in the formation of framboids and blocky pyrite in the 1.0% and 10% Fe-supplemented vessels, respectively (Fig. 12).

In summary, Ediacaran-style elemental maps demonstrated spatial associations between Ca and Mg, Ca and Al, and Fe and Al when additional Fe was not incorporated into the sediment before decaying the organisms. In the presence of supplemental reduced Fe, pyrite framboids and blocky pyrite precipitated on the surface of sediment grains proximal to the carcasses. This was apparent for sediment from the 'dirty' halos, as well as the intersection between halo and 'clean' sand.

DISCUSSION

Do Ediacaran-Style Taphonomic Scenarios Affect the 'Normal' (i.e., Open Marine) Pattern and Rate of Decay?—Patterns of decay were almost identical between baseline decay experiments and Ediacaran-style decay experiments in both organisms. Notable exceptions to this were observed with respect to the 'outer dermal' and 'gut' characters. In the baseline experiments, the outer dermal layer in sea anemones was more susceptible to decay than the 'gut' character, but under Ediacaran-style conditions, this character became less susceptible, and persisted longer than the 'gut'. In sea hares an opposite pattern was observed; the outer dermal layer in this organism was more susceptible to decay in the Ediacaran-style conditions than the baseline conditions. However, in Ediacaran-style conditions, the 'gut' of the sea hare decayed more quickly than the outer dermal layer, particularly the transition from DS3 to DS4. The fact that the outer dermal layer persisted longer than the 'gut' in Ediacaran-style experiments, in both anemones and sea hares, has important implications for the interpretation of Ediacaran fossils (discussed below).

Although patterns of decay were broadly similar in the two experiments, rates of decay were slower in Ediacaran-style experiments as compared to baseline experiments (Figs. 5, 9). In both sea anemones and sea hares, the least structurally complex tissues were first to transition from early decay stages to later decay stages. Sea anemone tentacles are the thinnest tissues of either decay organism, and in both experiments this character was lost more rapidly than any other character with the exception of the 'gut' in the sea hares. The rapid decay of tentacles is likely due to their tissue structure and histology; as fluid-filled sacs with large surface area, these tissues intuitively decompose more readily than thicker, less labile tissues such as the thick body tissues of the anemones. Counter to what we expected, tentacles in baseline experiments persisted longer than those subjected to Ediacaran-style conditions. This is plausibly a result of the large starting consortium of bacteria present in the microbial mats that could facilitate early decay of labile tissues. This observation has implications when interpreting fossils that might have a cnidarian- or actinian-affinity (for example, in the Ediacaran). As tentacles are more susceptible to being lost in Ediacaran-style taphonomic scenarios, there is a strong possibility that they are under-represented in Ediacaran fossil deposits (as compared deposits such as Mazon Creek which preserve tentacles), thus removing valuable anatomical and ecological information, and hindering future fossil interpretation.

Do Equivalent FeS 'Death Masks' Form With Both Sea Hares and Sea Anemones?—In our Ediacaran-style experiments (those without supplemented Fe), there was little evidence to support FeS 'death masks' forming in either our sea anemones or sea hares. Although we did see slower decay under Ediacaran-style conditions, we did not observe a spatial association between Fe and S in the EDS data (Fig. 3), in contrast to the experiments performed by Darroch et al. (2012). Firstly, it is unlikely that the limiting reagent in our experiment was sulfate. Ediacaran seawater is

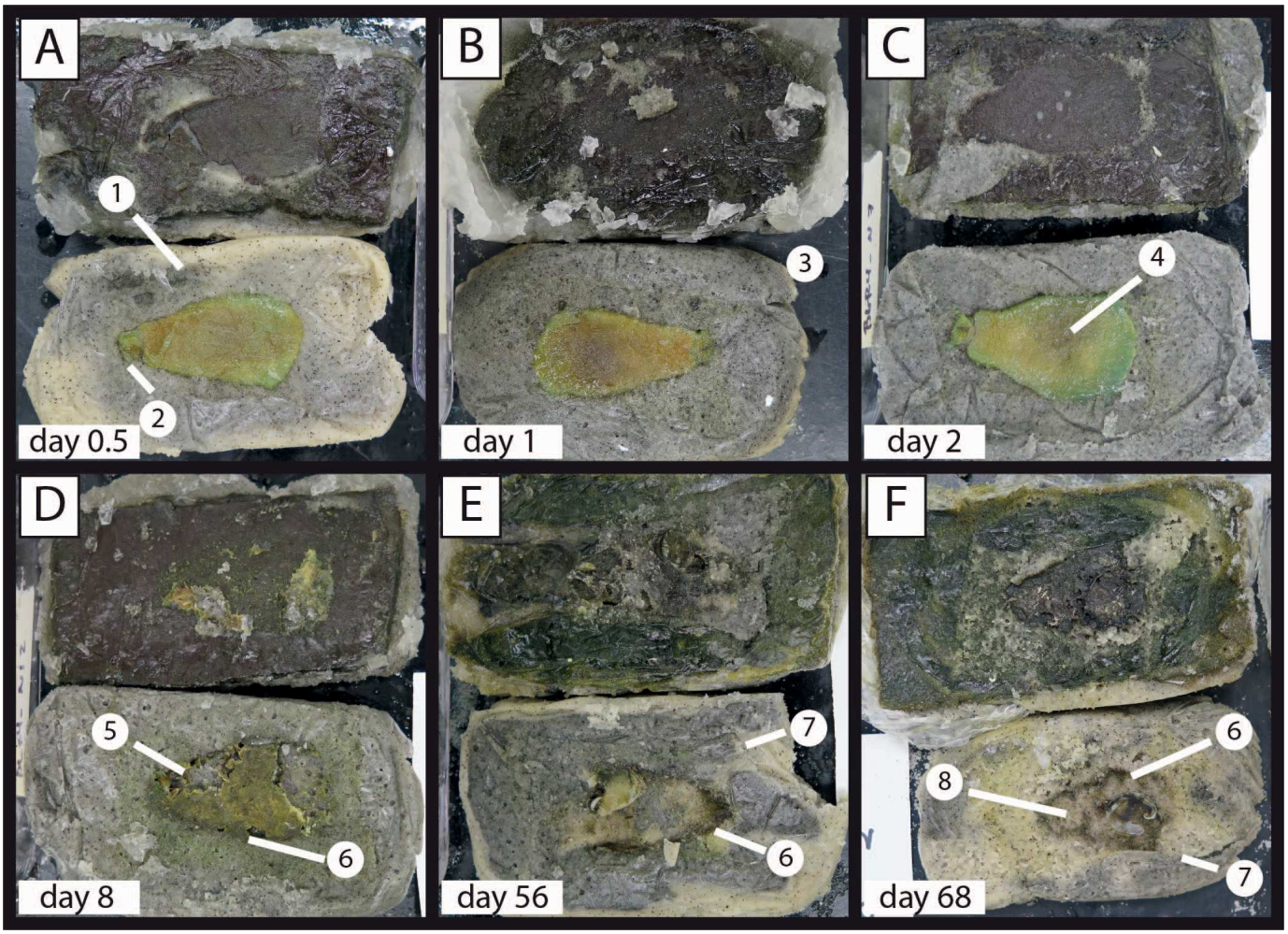

FIG. 10.—Progression of decay for wedge sea hare, *Dolabella auricularia*, under Ediacaran-style decay conditions. **A**) Emergence of decay 'halo' black precipitate. Precipitate front at [1] and anterior portion at [2]. **B**) Sea hare removed after 24 hours. Black precipitate halo encompassed decay vessel entirely [3]. **C**) Discoloration from internal gut decay shown at [4]. **D**) Internal gut mostly removed with persistence of outer dermal layer and muscle [5] while outline of carcass persists [6]. **E**) Decay halo begins to retract [7]. **F**) Cavity where carcass has entirely decayed [8] with some organic matter remaining via sediment staining [6]. "Halo" retracting from vessel edge [7].

thought to have had sulfate levels possibly two orders of magnitude lower than at present (Hayes et al. 1992; Canfield 1998; Shen et al. 2002; Shen et al. 2003; Poulton et al. 2004; Shen et al. 2008), which is not reflected in our use of Instant Ocean artificial seawater to saturate experiments. In contrast, our sediments and ASW were low in Fe, which implies that 'death mask' style preservation is reliant on a minimum level of available reactive iron, and that higher concentrations of Fe will produce better 'death masks' and (presumably) higher fidelity preservation. This is supported to some extent by the Fe-supplemented Ediacaran-style experiment results. With the addition of reduced Fe into the sediment, pyrite framboids were able to precipitate at the middle concentration (1.0%) of additional Fe provided in our experimental protocol. However, we note that higher concentrations of available Fe may not necessarily be conducive to preserving high-fidelity fossils. Above a certain threshold (between 1% and 10% of our sulfate levels), blocky cuboid pyrite becomes the dominant observed crystal structure.

Are the Dark Decay 'Halos' Consistently Associated with the Precipitation of Aluminosilicate Elements?—Darroch et al. (2012) noted a higher concentration of aluminosilicate elements within black decay 'halos' around decaying *G. mellonella* larvae than within the 'clean' sand outside it, and used this to suggest that authigenic clay mineral formation may have be an important component of Ediacaran preservation, serving to mold the external morphology of the carcass and create an impermeable barrier preventing diffusion oxygenated pore fluids. Although our decay EDS data are more variable, we note increased Al concentrations in decay 'halos' around carcasses, once carbon is removed (see online Supplemental file). Although removing carbon and re-normalizing adds

→

FIG. 11.—Elemental abundances of "clean" and "dirty" sediment from the decay vessels (e.g., sediment outside or within the decay halo, respectively). Boxplots show comparisons between "clean" (gray) and "dirty" (white) sediments for individual elements. Elements displayed are Fe (red); S (green); Mg (purple); K (light blue); Al (pink); and Ca (dark blue). Fe and S are plotted on secondary y-axis.

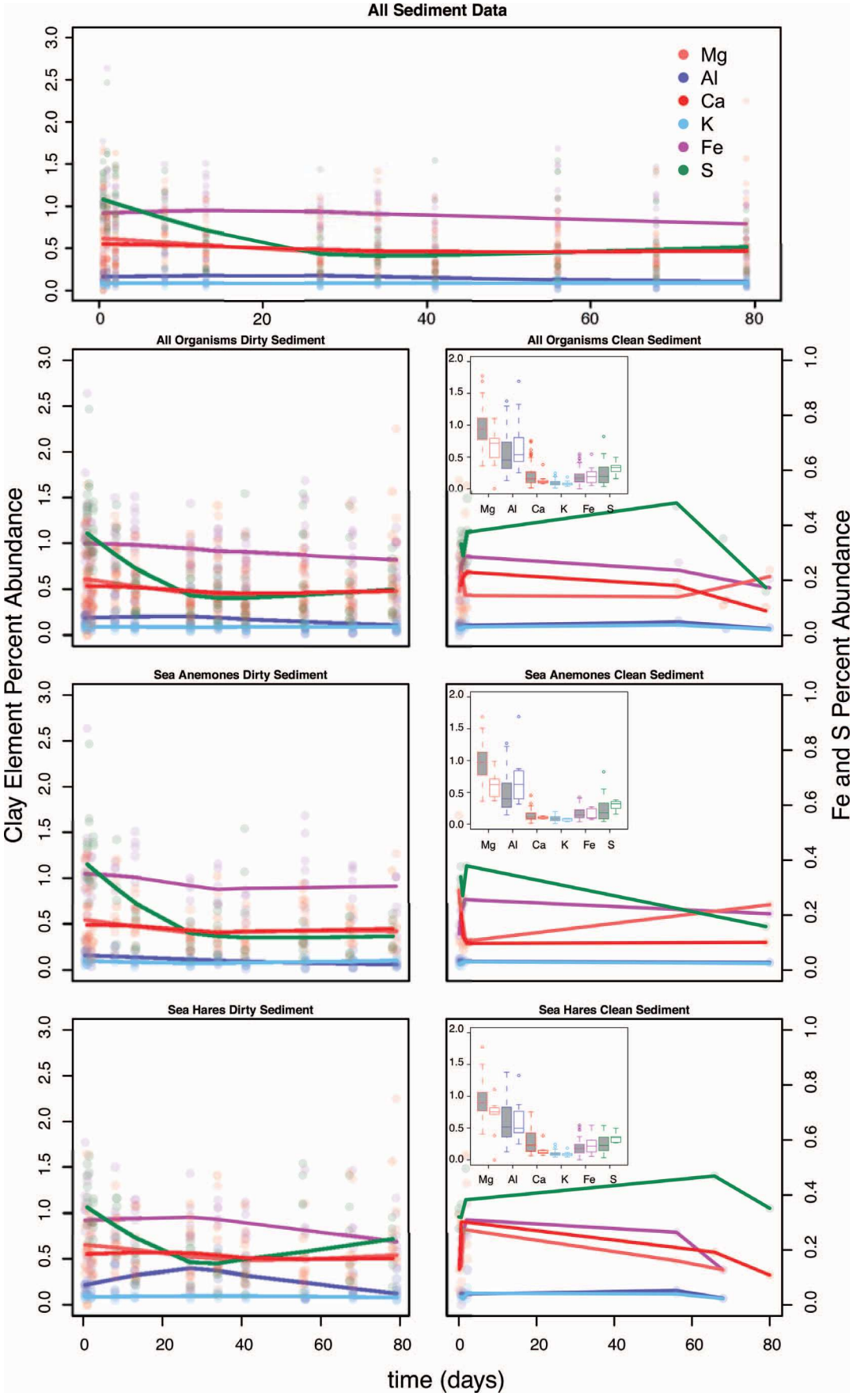
All Sediment Data
Mg
Al
Ca
K
Fe
S
All Organisms Dirty Sediment
All Organisms Clean Sediment
Sea Anemones Dirty Sediment
Sea Anemones Clean Sediment
Sea Hares Dirty Sediment
Sea Hares Clean Sediment
Clay Element Percent Abundance
Fe and S Percent Abundance
time (days)

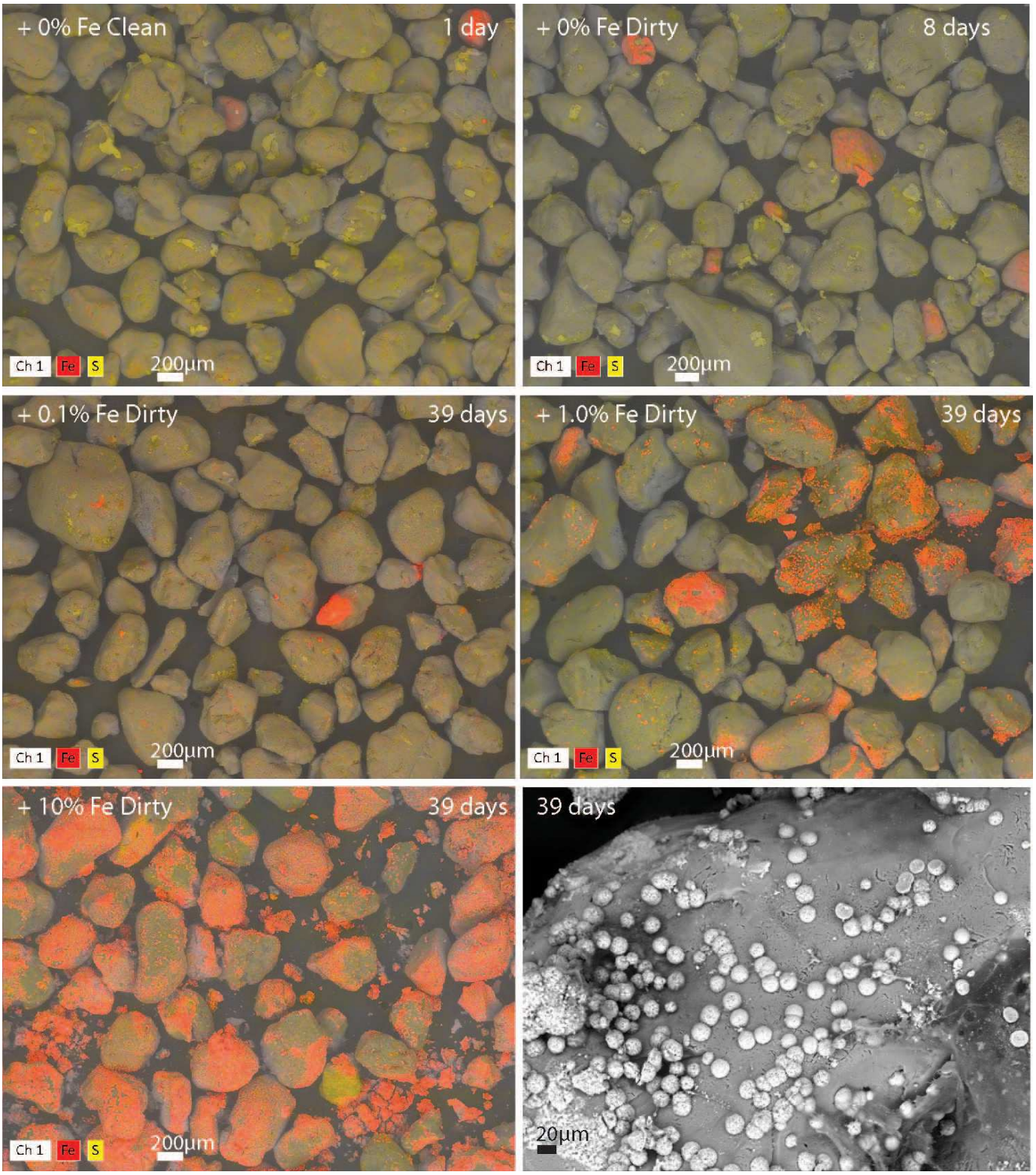

FIG. 12.—Iron supplemented decay sediment. As supplemental Fe concentration increases, FeS spatially associated. At 0.1%, few pyrite framboids precipitate on sediment. At 1.0% pyrite framboids dominate FeS associations. At 10% pyrite framboids are overprinted by "blocky" pyrite. Bottom right shows high magnification view of pyrite framboids.

more noise, stronger patterns associated with elements with lower abundance percentages begin to emerge. Specifically, Al typically fluctuates a bit more for the duration of the experiment, and it begins to increase in concentration towards the end (see online Supplemental file). Despite that, these increases and fluctuations are not substantial enough to definitively state that aluminosilicate precipitation is high in the vicinity of the carcasses (i.e., within the halos), relative to 'clean' sand.

We did not note obvious clay element aggregation within the Fe-supplemented decay sediments. Most of spatial associations between Al, Ca, and Mg were found to be qualitatively similar between clean and 'dirty' sediment. This indicates that clays may not be as important in controlling taphonomy within our experimental setup.

What is the Rate and Pattern of Aluminosilicate Precipitation as Decay Progresses?—When carbon is removed and the data are re-normalized, Al (as a proxy for bulk aluminosilicate) abundance initially decreases inside the decay halo in all samples, and then subsequently increases. This increase is not persistent in all sediment bins, as no increase is noted from sediment collected from the edge of the decay vessel during which the decay halo had completely encompassed the vessel in the anemone experiments (see online Supplemental file). The percentage coverage of K and Ca remain fairly constant throughout, with K maintaining almost 0% for the entire duration of the experiment. The only noticeable spatial association in EDS maps are between Fe and Al, and between Al and Ca. In sea hares, Al and Ca clump more than they do with anemones. This is likely due to the local enrichment of calcium from the posterior shell.

What is the Relative Importance of FeS Versus Clay Minerals in Molding the External Morphology of Carcasses, and thus in Fossil Preservation?—When looking for clay element co-occurrences in the EDS spatial maps, there is a greater degree of spatial association between aluminosilicate elements than observed with the Fe and S maps for the experiments which did not receive supplement Fe, but still not enough to suggest the formation of clay minerals. More interesting is the tight association of Fe and Al, which often overlap (Fig. 3). Fe more often occurs on sediment grains that have Al, than it does for areas of increased S. Previous work has demonstrated that biofilms (which typically have negatively charged surfaces) may attract positively charged elements (Ferris et al. 1989). It is conceivable that areas with increased Al in our sediment samples correspond to areas of increased biofilm production, something not specifically analyzed within this project. If this is demonstrated to be true, then Al and Fe association could potentially be used as a proxy for biofilm production, but this should be tested much more rigorously before being used as such. More importantly, the FeS spatial associations in the form of pyrite framboids (Fig. 12) from Fe-supplemented experiments demonstrate that pyrite precipitates early within the taphonomic window (within weeks). While associations between Fe and S increase, associations between aluminosilicate elements do not. What should be tested more rigorously in future studies is the effects of additional dissolved silica within the seawater on the accumulation of clays (Newman et al. 2016a, 2016b). Our experimental design did not include dissolved silica within the ASW but could easily be modified to do so. This would then provide a clearer test for the relative importance of clay minerals versus FeS in Ediacaran-style preservation.

Broader Implications

The results of these experiments have implications both for the interpretation of Ediacaran fossils, as well as the efficacy of the pyritic 'death mask' model for Ediacaran fossil preservation. For interpreting Ediacaran fossils, the observation that the decay of key characters (the tentacles of sea anemones, and the 'guts' of both sea hares in particular) are not clearly slowed in Ediacaran-style taphonomic scenarios (and in some cases, decay even faster than in baseline 'open' conditions), suggests that these characters are unlikely to be recognized in Ediacaran fossil assemblages, even if they were originally present. In other words, our experiments show that Ediacaran 'death mask' conditions bias against key actinian and molluscan characters that would typically be used to constrain the phylogenetic affinity of fossils. More specifically, the rapid decay of tentacles in our sea anemone experiments illustrates that Ediacaran preservational pathways may confound reliable interpretation of fossils as actinian-grade cnidarians, and could be affecting our interpretation of preferred feeding strategies if these structures are lost early in decay.

Although developed with Ediacaran preservation in mind, our indices can also be used to interpret younger soft-bodied fossils. We tested the utility of our indices and comparative decay patterns outside the Ediacaran by looking at the Cambrian organism *Mackenzia*, which has been interpreted as an anemone of the earliest Phanerozoic (Conway Morris 1993a, 2000) and should possess some classic anemone characteristics if previous reconstructions are indeed correct. Figure 13 also incorporates *Mackenzia* specimens that show similarities with our anemone experimental data. Figure 13-E shows long, dark bands running the length of the organism. Such bands are markedly similar to the mesenteries of modern sea anemones, a feature not found in other organisms. The posterior portion of the organism has a very discrete bulbous end, which looks similar to the holdfasts of Ediacaran fronds, or the pedicle foot of anemones. Our assessment concurs with previous interpretations of *Mackenzia* as an anemone. Specimens of *Mackenzia* have not been collected with evidence of tentacles, but if such features were present they would likely have been lost in early decay, even under conditions favorable to soft-tissue preservation, as our decay experiments have demonstrated. We would also like to note the similarities with *Inaria* (Fig. 13). Fossil *Inaria* are often garlic-shaped with dark, crevice-like structures running from the exterior of the fossil towards the center. These crevice-like structures appear similar to the mesenteries of anemones, similar to the dark bands noted on *Mackenzia*. Furthermore, *Inaria* fossils exhibit the same "folding over" pattern that our anemones did during the Ediacaran-style decay experiments. The thin anterior portion of *Inaria* often is observed to have folded over the bulbous bottom portion. This appears markedly similar to the body column of the anemones folding over their respective "foot".

Results from sea hare experiments also have implications for the fossil record, specifically interpreting Ediacaran fossils. The 'gut' of the sea hares in our decay experiments rapidly disappeared leaving just an outline of the carcasses in the form of the outer most dermal layer. The Ediacaran organism *Kimberella quadrata* (Glaessner and Wade 1966; Fig. 13) has

→

FIG. 13.—Comparison of decay organisms from this study, and three Ediacaran or Cambrian fossils. **A**) Sea anemone from Ediacaran-style decay experiment showing persistence off all anatomy. **B**) Decay index for anemone generated from this study. **C**) Ediacaran fossil *Inaria* (specimen S.A. Museum P27917) of South Australia. **D**) *Kimberella* of White Sea Assemblage showing enhanced 3-D preservation. **E**) Cambrian fossil *Mackenzia* (specimen NMNH PAL 57557), rotated view showing interpreted mesenteries. Key: 1 = mesentery tissue of anemone; 2 = cavity left from decay; 3 = folds in tissue of *Inaria*; 4 = possible cavity from decay in *Kimberella*; 5 = possible mesenteries of *Mackenzia*.

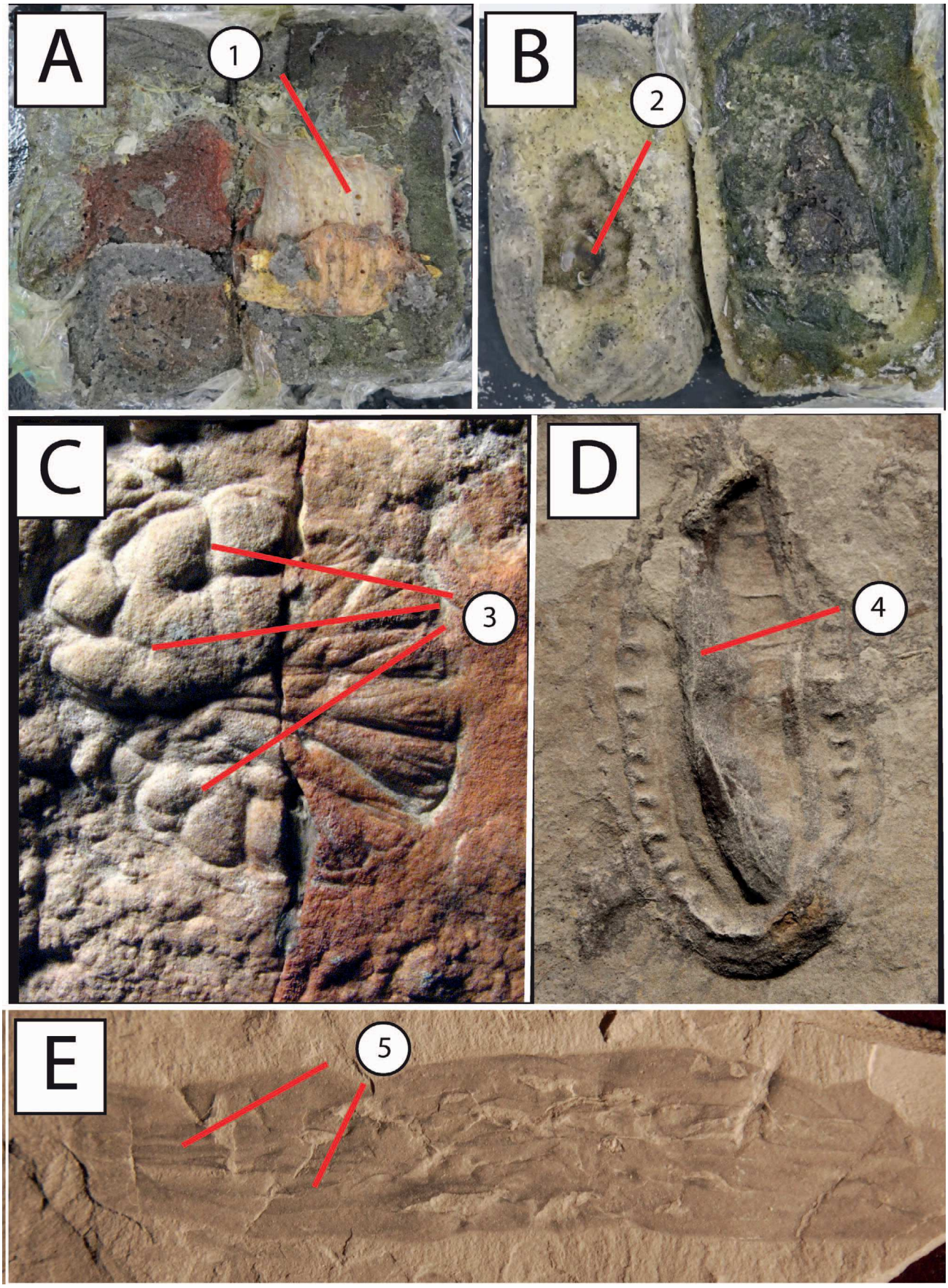
A
1
B
2
C
3
D
4
E
5

been interpreted as a stem-group mollusk (Fedonkin 2003; Fedonkin et al. 2007; Seilacher 2007; Ivantsov 2009; Gehling et al. 2014), but this interpretation has been challenged (Erwin 1999). One of the strongest arguments against *Kimberella* as a mollusk is the lack of hemocoel, which all mollusks possess. According to Erwin (1999), if *Kimberella* were indeed a triploblast and mollusk, it would have had this fluid-filled cavity. Given the results of our decay experiments, this key molluscan feature is lost rapidly within the taphonomic window, implying that *Kimberella* would most likely lose evidence of this feature.

Lastly, in terms of the pyritic 'death mask' model for Ediacaran fossilization, our decay organisms produced the pyrite framboids necessary for the classic Gehling (1999) 'death mask' model when additional Fe was added into our Fe-limited sediment. These results indicate that pyrite will form early within the taphonomic window preserving soft-bodied organisms, and likely explains preserved pyrite and associated weathering products known from the rock record. If Fe is the principal limiting reagent in Ediacaran-style 'death mask' formation, then this might suggest that this taphonomic pathway is specific to certain facies and/or tectonic settings, and thus that the Ediacaran fossil record possesses some degree of facies or paleogeographic bias. However, we also acknowledge that there may have been multiple taphonomic pathways to preserving Ediacaran organisms in the latest Neoproterozoic. In these experiments we demonstrate key tenets of the pyritic 'death mask' model, however, only further experiments (e.g., incorporating elevated concentrations of dissolved silica—see Tarhan et al. 2016) will establish whether this was the only process responsible for preserving Ediacaran organisms, or whether multiple pathways were operating in different localities. Our experimental design can easily be adjusted to test these alternative taphonomic pathways.

CONCLUSIONS

The results from our experiments illustrate that, although the overall pattern of decay is broadly similar in both baseline and Ediacaran-style experiments, the rates of decay in Ediacaran experiments are much slower overall, while also apparently accelerating the decay of certain phylogenetically important characters. In addition, slight differences in the patterns of decay between the two sets of experiments reveal that Ediacaran taphonomic scenarios potentially bias against the preservation of key diploblastic and triploblastic characters. Although outer dermal layers persist for long periods of time resulting in a clear outline of the organism, little in the way of internal or labile delicate external anatomy is likely to survive. This suggests that many enigmatic Ediacaran fossils could equally represent either diploblastic or triploblastic organisms, and that the taphonomic pathway may effectively prevent us from distinguishing between the two. This is in contrast to the interpretations provided in McMahon et al. (2017), who argue that these two groups should be distinguishable based on the persistence of *Metridium* muscles in their decay experiments, which should be outlasted by triploblastic features. More studies are required over a larger range of diploblastic and triploblastic organisms to fully assess this relationship.

Our experiments also illustrate that the black 'decay halo' that precipitates outward from decaying carcasses in Ediacaran-style experiments does not correspond to either FeS or aluminosilicate precipitation. Although additional analyses should be conducted, we hypothesize that this enrichment of dark sand corresponds to increase organics dispersing from the carcass as it decays. Regardless, more work is required to better understand the direct relationship between the different interpretations of 'death mask' style preservation and this halo.

Most importantly, our results demonstrate the likelihood of the pyritic 'death mask' preservation model functioning during the Ediacaran. Furthermore, we demonstrate there is an upper limit to Fe concentrations after which it is unlikely that fine-scale anatomy will be preserved.

ACKNOWLEDGMENTS

This project was made possible through generous support to BMG from the Geological Society of America (Graduate Student Research Grant), a Paleontological Society Student Grant (Harry B. Whittington Award), and a Sigma Xi Grant-in-Aid of Research Award. JDS is supported by NSF EAR CAREER-1652351, and acknowledges support of the X-ray Microanalysis Core Facility by NSF EAR I&F-1636643. BMG and SAFD would like to thank Neil Kelley for helpful comments and edits to an earlier draft. All authors would like to thank Sean McMahon and an anonymous reviewer, who provided constructive criticism which considerably improved an earlier draft of this manuscript.

SUPPLEMENTAL MATERIAL

Data are available from the PALAIOS Data Archive: http://www.sepm.org/pages.aspx?pageid=332.

REFERENCES

Anderson, E.P., Schiffbauer, J.D., and Xiao, S., 2011, Taphonomic study of Ediacaran organic-walled fossils confirms the importance of clay minerals and pyrite in Burgess Shale-type preservation: Geology, v. 39, p. 643–646, doi: 10.1130/G31969.1.

Briggs, D.E.G., 2003, The role of decay and mineralization in the preservation of soft-bodied fossils: Annual Review of Earth and Planetary Sciences, v. 31, p. 275–301, doi: 10.1146/annurev.earth.31.100901.144746.

Briggs, D.E.G. and McMahon, S., 2016, The role of experiments in investigating the taphonomy of exceptional preservation: Palaeontology, v. 59, p. 1–11, doi: 10.1111/pala.12219.

Brusca, R.C., 1980, Common Intertidal Invertebrates of the Gulf of California: University of Arizona Press, Tucson, p. 513.

Buss, L.W. and Seilacher, A., 1994, the Phylum Vendobionta—a Sister Group of the Eumetazoa: Paleobiology, v. 20, p. 1–4, doi: 10.2307/2401145.

Butterfield, N.J., 1995, Secular distribution of Burgess Shale-type preservation: Lethaia, v. 28, p. 1–3, doi:10.1111/j.1502-3931.1995.tb01587.x.

Callow, R.H.T. and Braiser, M.D., 2009, Remarkable preservation of microbial mats in Neoproterozoic siliciclastic settings: implications for Ediacaran taphonomic models: Earth-Science Reviews, v. 96, p. 207–219, doi: 10.1016/j.earscirev.2009.07.002.

Canfield, D.E., 1998, A new model for Proterozoic ocean chemistry: Nature, v. 396, p. 450–453, doi: 10.1038/24839.

Cameron, C.B., 2002, Particle retention and flow in the pharynx of the enteropneust worm *Harrimania planktophilus*: the filter-feeding pharynx may have evolved before the chordates: Biological Bulletin, v. 202, p. 192–200.

Casenove, D., Oji, T., and Goto, T., 2011, Experimental taphonomy of benthic chaetognaths: implications for the decay process of Paleozoic chaetognath fossils: Paleontological Research, v. 15, p. 146–153, doi: 10.2517/1342-8144-15.3.146.

Conway Morris, S., 1993a, Ediacaran-like fossils in Cambrian Burgess shale-type faunas of North America: Palaentology, v. 36, p. 593–635.

Conway Morris, S., 1993b, The fossil record and the early evolution of the Metazoa: Nature, v. 361, p. 219–225, doi: 10.1038/361219a0.

Conway Morris, S., 2000, The Cambrian "explosion": slow-fuse or megatonnage?: Proceedings of the National Academy of Sciences of the United States of America, v. 97, p. 4426–4429, doi: 10.1073/pnas.97.9.4426.

Cui, H., Kaufman, A.J., Xiao, S., Peek, S., Cao, H., Min, X., Cai, Y., Siegel, Z., Liu, X., Peng, Y., Schiffbauer, J.D., and Martin, A.J., 2016, Environmental context for the terminal Ediacaran biomineralization of animals: Geobiology, v. 14, p. 344–363, doi: 10.1111/gbi.12178.

Darroch, S.A.F., Laflamme, M., SchiffbauerJ. D., and Briggs, D.E.G., 2012, Experimental formation of a microbial death mask: PALAIOS, v. 27, p. 293–303, doi: 10.2110/palo.2011.p11-059r.

Darroch, S.A.F., Sperling, E.A., Boag, T.H., Racicot, R.A., Mason, S.J., Morgan, A.S., Tweedt, S., Myrow, P., Johnston, D.T., Erwin, D.H., and Laflamme, M., 2015, Biotic replacement and mass extinction of the Ediacara biota: Proceedings of the Royal Society B, v. 282, 20151003.

Droser, M.L., Gehling, J.G., and Jensen, S.R., 2006, Assemblage palaeoecology of the Ediacara biota: the unabridged edition?: Palaeogeography, Palaeoclimatology, Palaeoecology, v. 232, p. 131–147, doi: 10.1016/j.palaeo.2005.12.015.

Erwin, D.H., 1999, The origin of bodyplans: American Zoologist, v. 39, p. 617–629.

Erwin, D.H., Laflamme, M., Tweedt, S.M., Sperling, E A., Pisani, D., and Peterson, K.J., 2011, The Cambrian Conundrum: early divergence and later ecological success in the early history of animals: Science, v. 334, p. 1091–1097, doi: 10.1126/science.1206375.

Fedonkin, M.A., 2003, The origin of the Metazoa in the light of the Proterozoic fossil record: Paleontological Research, v. 7, p. 9–41.

Fedonkin, M.A., Simonetta, A., and Ivantsov, A.Y., 2007, New data on *Kimberella*, the Vendian mollusk-like organism (White Sea region, Russia): palaeoecological and evolutionary implications: Geological Society, London, Special Publications, v. 286, p. 157–179, doi: 10.1144/SP286.12.

Fedonkin, M.A. and Waggoner, B.M., 1997, The late Precambrian fossil *Kimberella* is a mollusc-like bilaterian organism: Nature, v. 388, p. 868–871, doi: 10.1038/42242.

Ferris, F.G., Schultze, S., Witten, T.C., Fyfe W.S., and Beveridge, T.J., 1989, Metal interactions with microbial biofilms in acidic and neutral pH environments: Applied and Environmental Microbiology, v. 55, p. 1249–1257.

Gehling, J.G., 1988, A cnidarian of actinian-grade from the Ediacaran Pound Subgroup, South Australia: An Australasian Journal of Palaeontology, v. 12, p. 299–314, doi: 10.1080/03115518808619129.

Gehling, J.G., 1991, The case of Ediacaran fossil roots to the metazoan tree: Memoirs, Geological Society of India, v. 20, p. 181–224.

Gehling, J.G., 1999, Microbial mats in terminal Proterozoic siliciclastics; Ediacaran death masks: PALAIOS, v. 14, p. 40–57, doi: 10.2307/3515360.

Gehling, J.G., Droser, M.L., Jensen, S.R., and Runnegar, B.N., 2005, Ediacara organisms: relating form to function, *in* D.E.G. Briggs (ed.), Evolving Form and Function: Fossils and Development, Proceedings of a Symposium Honoring Adolf Seilacher for His Contributions to Paleontology in Celebration of His 80th Birthday: Peabody Museum of Natural History, New Haven, Connecticut, p. 43–66.

Gehling, J.G., Runnegar, B.N., and Droser, M.L., 2014, Scratch traces of large Ediacara bilaterian animals: Journal of Paleontology, v. 88, p. 284–298, doi: 10.1666/13-054.

Glaessner, M.F. and Wade, M., 1966, The late Precambrian fossils from Ediacara, South Australia: Palaeontology, v. 9, p. 599–628.

Hayes, J.M., Lambert, I.B., and Strauss, H., 1992, The sulfur-isotopic record, *in* J.W. Schopf and C. Klein (eds.), The Proterozoic Biosphere: A Multidisciplinary Study: Cambridge University Press, Cambridge, p. 129–131.

Hofmann, H.J., Narbonne, G.M., and Aitken, J.D., 1990, Ediacaran remains from intertillite beds in northwestern Canada: Geology, v. 18, p. 1199–1202, doi: 10.1130/0091-7613(1990)018<1199:ERFIBI>2.3.CO;2.

Ivantsov, A.Y., 2009, New reconstruction of *Kimberella*, problematic Vendian metazoan: Paleontological Journal, v. 43, p. 601–611, doi: 10.1134/S003103010906001X.

Laflamme, M. and Narbonne, G.M., 2008, Ediacaran fronds: Palaeogeography, Palaeoclimatology, Palaeoecology, v. 258, p. 162–179, doi: 10.1016/j.palaeo.2007.05.020.

Laflamme, M., Schiffbauer, J.D., Narbonne, G.M., and Briggs, D.E.G., 2011, Microbial biofilms and the preservation of the Ediacara biota: Lethaia, v. 44, p. 203–213, doi: 10.1111/j.1502-3931.2010.00235.x.

Leary, S., Underwood, W., Anthony, R., and Cartner, S., 2013, AVMA Guidelines for the Euthanasia of Animals, 2013 edition: American Veterinary Medical Association, Schaumburg, IL, 98 p.

Liu, A.G., Kenchington, C.G., and Mitchell, E.G., 2015, Remarkable insights into the paleoecology of the Avalonian Ediacaran macrobiota: Gondwana Research, v. 27, p. 1355–1380, doi: 10.1016/j.gr.2014.11.002.

Liu, A.G., Matthews, J.J., and McIlroy, D., 2016, The Beothukis/Culmofrons problem and its bearing on Ediacaran macrofossil taxonomy: evidence from an exceptional new fossil locality: Palaeontology, v. 59, p. 45–58, doi: 10.1111/pala.12206.

Mapstone, N.B. and McIlroy, D., 2006, Ediacaran fossil preservation: taphonomy and diagenesis of a discoid biota from the Amadeus Basin, central Australia: Precambrian Research, v. 149, p. 126–148, doi: 10.1016/j.precamres.2006.05.007.

McMahon, S., Tarhan, L.D., and Briggs. D.E.G., 2017, Decay of the sea anemone Metridium (Actiniaria): implications for the preservation of cnidarian polyps and other soft-bodied diploblast-grade animals: PALAIOS, v. 32, p. 388–395, doi: 10.2110/palo.2016.102.

Meyer, M., Elliott, D., Schiffbauer, J.D., Hall, M., Hoffman, K.H., Schneider, G., Vickers-Rich, P., and Xiao, S., 2014, Taphonomy of the Ediacaran fossil Pteridinium simplex preserved three-dimensionally in mass flow deposits, Nama Group, Namibia: Journal of Paleontology, v. 88, p. 240–252, doi: 10.1666/13-047.

Meyer, M., Schiffbauer, J.D., Xiao, S., Cai, Y., and Hua, H., 2012, Taphonomy of the upper Ediacaran enigmatic ribbonlike fossil Shaanxilithes: PALAIOS, v. 27, p. 354–372, doi: 10.2110/palo.2011.p11-098r.

Nanglu, K., Caron, J.-B., and Cameron, C.B., 2015, Using experimental decay of modern forms to reconstruct the early evolution and morphology of fossil enteropneusts: Paleobiology, v. 41, p. 460–478, doi: 10.1017/pab.2015.11.

Narbonne, G.M., 2005, The Ediacara biota: Neoproterozoic origin of animals and their ecosystems: Annual Review of Earth and Planetary Sciences, v. 33, p. 421–442, doi: 10.1146/annurev.earth.33.092203.122519.

Newman, S.A., Mariotti, G., Pruss, S., and Bosak, T., 2016a, Insights into cyanobacterial fossilization in Ediacaran siliciclastic environments: Geology, v. 44, p. 579–582, doi: 10.1130/G37791.1.

Newman, S.A., Vlepac-Ceraj, V., Mariotti, G., Pruss, S.B., Watson, N., and Bosak, T., 2016b, Experimental fossilization of mat-forming cyanobacteria in coarse-grained siliciclastic sediments: Geobiology, v. 15, p. 484–498, doi: 10.1111/gbi.12229.

Noffke, N., 2010, Geobiology: Microbial Mats in Sandy Deposits from the Archean Era to Today: Springer-Verlag, Berlin, 194 p.

Noffke, N., Knoll, A.H., and Grotzinger, J.P., 2002, Sedimentary controls on the formation and preservation of microbial mats in siliciclastic deposits: a case study from the upper Neoproterozoic Nama Group, Namibia: PALAIOS, v. 17, p. 533–544, doi: 10.1669/0883-1351(2002)017<0533:SCOTFA>2.0.CO;2.

Norris, R.D., 1989, Cnidarian taphonomy and affinities of the Ediacara biota: Lethaia, v. 22, p. 381–393, doi: 10.1111/j.1502-3931.1989.tb01439.x.

Orr, P.J., Briggs, D.E.G., and Kearns, S.L., 1998, Cambrian Burgess Shale animals replicated in clay minerals: Science, v. 281, p. 1173–1175, doi: 10.1126/science.281.5380.1173.

Park, E., Hwang, D.S., Lee, J.S., Song, J.I., Seo, T.K., and Won, Y.J., 2012, Estimation of divergence times in cnidarian evolution based on mitochondrial protein-coding genes and the fossil record: Molecular Phylogenetics and Evolution, v. 62, p. 329–345, doi: 10.1016/j.ympev.2011.10.008.

Pek, I., Vašíček, Z., Roček, Z., Hajn, V., and Mikuláš, R., 1996, Základy Zoopaleontologie: Vydavatelství Univerzity Palackého, Olomouc, 264 p.

Peterson, K.J., Wagonner, B., and Hagadorn, J.W., 2003, A fungal analog for newfoundland Ediacaran fossils?: Integrative and Comparative Biology, v. 43, p. 127–36, doi: 10.1093/icb/43.1.127.

Poulton, S.W., Fralick, P.W., and Canfield, D.E., 2004, The transition to a sulphidic ocean ~1.84 billion years ago: Nature, v. 431, p. 173–177, doi: 10.1038/nature02912.

Retallack, G.J., 1994, Were the Ediacaran fossils lichens?: Paleobiology, v. 20, p. 523–544.

Sansom, R.S., Gabbott, S.E., and Purnell, M.A., 2010, Non-random decay of chordate characters causes bias in fossil interpretation: Nature, v. 463, p. 797–800, doi: 10.1038/nature08745.

Sansom, R.S., Gabbott, S.E., and Purnell, M.A., 2011, Decay of vertebrate characters in hagfish and lamprey (Cyclostomata) and the implications for the vertebrate fossil record: Proceedings, Biological Sciences, The Royal Society, v. 278, p. 1150–1157, doi: 10.1098/rspb.2010.1641.

Sansom, R.S. and Wills, M.A., 2013, Fossilization causes organisms to appear erroneously primitive by distorting evolutionary trees: Scientific Reports, v. 3, article 2545, p. 1–5, doi: 10.1038/srep02545.

Schiffbauer, J.D., Xiao, S., Cai, Y., Wallace, A.F., Hua, H., Hunter, J., Xu, H., Peng, Y., and Kaufman, A.J., 2014, A unifying model for Neoproterozoic–Palaeozoic exceptional fossil preservation through pyritization and carbonaceous compression: Nature Communications, v. 5, p. 5754, doi: 10.1038/ncomms6754.

Seilacher, A., 1989, Vendozoa: organismic construction in the Proterozoic biosphere: Lethaia, v. 22, p. 229–239.

Seilacher, A., 1999, Biomat-related lifestyles in the Precambrian: PALAIOS, v. 14, p. 86–93, doi: 10.2307/3515363.

Seilacher, A., 2007, Trace Fossil Analysis: Springer Verlag, Berlin Heidelberg New York, 226 p.

Seilacher, A., Grazhdankin, D., and Legouta, A., 2003, Ediacaran biota: the dawn of animal life in the shadow of giant protists: Paleontological Research, v. 7, p. 43–54, doi: 10.2517/prpsj.7.43.

Seilacher, A. and F. Pflüger, 1994, From biomats to benthic agriculture: a biohistoric revolution, *in* W.E. Krumbein and L.J. Stal (eds.), Biostabilization of Sediments: Bibliotheks und Informations system der Carl von Ossietzky Universität, Oldenburg, p. 97–105.

Shen, B., Dong, L., Xiao, S., and Kowalewski, M., 2008, The Avalon Explosion: evolution of Ediacaran morphospace: Science, v. 319, p. 81–84, doi: 10.1126/science.1150279.

Shen, Y., Canfield, D.E., and Knoll, A.H., 2002, Middle Proterozoic ocean chemistry: evidence from the McArthur Basin, northern Australia: American Journal of Science, v. 302, p. 81–109, doi: 10.2475/ajs.302.2.81.

Shen, Y., Knoll, A.H., and Walter, M.R., 2003, Evidence for low sulphate and anoxia in a mid-Proterozoic marine basin: Nature, v. 423, p. 632–635, doi: 10.1038/nature01651.

Sokolov, B.S. and Fedonkin, M.A., 1984, The Vendian as the terminal system of the Precambrian: Episodes Journal of International Geoscience, v. 7, p. 12–19.

Steiner, M. and Reitner, J., 2001, Evidence of organic structures in Ediacara-type fossils and associated microbial mats: Geology, v. 29, p. 1119–1122, doi: 10.1130/0091-7613(2001)029<1119.

Tarhan, L.G., Droser, M.L., and Gehling, J.G., 2015, Depositional and preservational environments of the Ediacara Member, Rawnsley Quartzite (South Australia): assessment of paleoenvironmental proxies and the timing of "ferruginization": Palaeogeography, Palaeoclimatology, Palaeoecology, v. 434, p. 4–13, doi: 10.1016/j.palaeo.2015.04.026.

Tarhan, L.G., Hood, A.v.S., Droser, M.L., Gehling, J.G., and Briggs, D.E.G., 2016, Exceptional preservation of soft-bodied Ediacara Biota promoted by silica-rich oceans: Geology, v. 44, p. 951–954, doi: 10.1130/G38542.1.

Tarhan, L.G., Hughes, N.C., Myrow, P.M., Bhargava, O.N., Ahluwalia, A.D., and Kudryavtsev, A.B., 2014, Precambrian–Cambrian boundary interval occurrence and form of the enigmatic tubular body fossil *Shaanxilithes ningqiangensis* from the Lesser Himalaya of India: Palaeontology, v. 57, p. 283–298, doi: 10.1111/pala.12066.

Vasconcelos, C., Warthmann, R., McKenzie, J.A., Visscher, P.T., Bittermann, A.G., and von Lith, Y., 2006, Lithifying microbial mats in Lagoa Vermelha, Brazil: Modern Precambrian relics?: Sedimentary Geology, v. 185, p. 175–183.

Vinther, J., 2015, The origins of molluscs: Palaeontology, v. 58, p. 19–34, doi: 10.1111/pala.12140.

Wade, M., 1968, Preservation of soft-bodied animals in Precambrian sandstones at Ediacara, South Australia: Lethaia, v. 1, p. 238–267, doi: 10.1111/j.1502-3931.1968.tb01740.x.

Xiao, S. and Laflamme, M., 2009, On the eve of animal radiation: phylogeny, ecology and evolution of the Ediacara biota: Trends in Ecology and Evolution, v. 24, p. 31–40, doi: 10.1016/j.tree.2008.07.015.

Zhuravlev, A.Y., 1993, Were Ediacaran Vendobionta multicellulars?: Neues Jahrbuch für Geologie und Paläontologie, Abhandlungen, v. 190, p. 299–314.

Received 17 October 2017; accepted 24 March 2018.